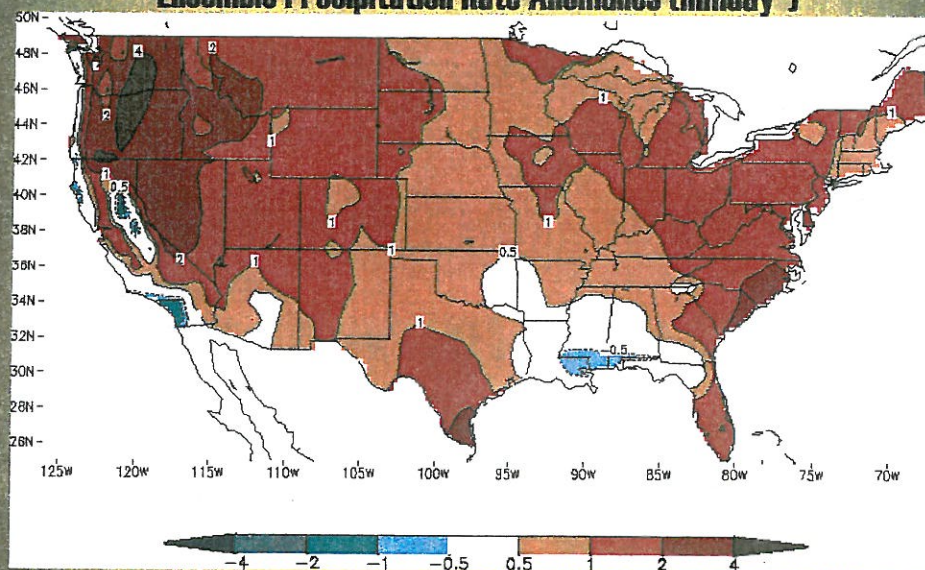# Winter Temperature and Precipitation Verification of the NCEP Operational Climate Model

by

David J. Salapata[1], Wayne Higgins[2], Jae-Kyung Schemm[2], and James J. O'Brien[1]

Ensemble Precipitation Rate Anomalies (mmday[-1])

[1] THE CENTER FOR OCEAN-ATMOSPHERIC PREDICTION STUDIES
THE FLORIDA STATE UNIVERSITY
TALLAHASSEE, FL USA 32306-2840

[2] NOAA/NCEP/NWS/CLIMATE PREDICTION CENTER
CAMP SPRINGS, MD USA 20746-4304

NOAA

COAPS

Florida State
UNIVERSITY

CENTER FOR OCEAN-ATMOSPHERIC PREDICTION STUDIES

THE FLORIDA STATE UNIVERSITY

TALLAHASSEE, FL 32306, USA

DIRECTOR: DR. JAMES J. O'BRIEN

WINTERTIME TEMPERATURE AND PRECIPITATION VERIFICATION

OF THE NCEP OPERATIONAL CLIMATE PREDICTION MODEL

By

DAVID J. SALAPATA

JAE-KYUNG SCHEMM

WAYNE HIGGINS

JAMES J. O'BRIEN

AUGUST, 2002

TECHNICAL REPORT

TABLE OF CONTENTS

ABSTRACT

The seasonal predictability of mean temperature and precipitation is evaluated for the operational National Centers for Environmental Prediction (NCEP) climate prediction model (see appendix). Hindcasts of 3-month climate forecasts with a 10-member ensemble are made during 1979-1999. Initial conditions are updated yearly. A simple diagnostic approach is taken to determine the ability of the model to predict seasonal temperature and precipitation patterns. Special attention is given to the ability to forecast patterns associated with El Nino Southern Oscillation (ENSO) and Arctic Oscillation (AO).

The 21-year mean of ensemble mean temperature for the January-March (JFM) season is shown to have a cold bias in the eastern United States, especially around the Great Lakes and Northeast, and there are cold biases in the Southwest. Model precipitation rates are higher than observations throughout the country. The only exceptions are along the northern Gulf coast and a narrow strip along the Pacific coast.

Prediction of temperature and precipitation anomalies associated with ENSO was poor but better for cold than for warm events. For cold events, temperature anomalies were forecasted well, although the magnitude of the anomaly differed in different regions. Precipitation anomaly predictions were poor for some events but improved over warm events for others. For warm events, anomaly patterns for both parameters on average were poorly represented in the model, although for some individual events

ii

anomalies were predicted accurately. With regard to the Arctic Oscillation, the model showed no skill in predicting patterns associated with negative and positive events. This result suggests the model is unable to predict or maintain low frequency modes in the atmosphere.

Finally, anomaly correlations for both seasonal mean temperature and precipitation were low with no regions of correlations greater than 0.5. Skill scores calculated in comparison with climatology are negative almost everywhere, indicating that model forecasts for both parameters are not an improvement over climatology. However, skill scores calculated in comparison with persistence show improvements in the Great Plains and Pacific Northwest for temperature and the northern Gulf states and California for precipitation.

1. INTRODUCTION

The climate of the U.S. varies on time scales ranging from monthly to decadal and longer. The ability to predict these changes is a challenge presented to the climate community. The goal is to create models that can accurately forecast climate variations. A consistently high degree of accuracy in seasonal forecasting is needed if a global climate model is to be a useful tool. Previous studies (e.g., Kumar et al. 1996) have shown that given accurate forecasts of certain long-lived boundary forcings useful seasonal climate predictions can be made for both the tropics and extratropics.

The difficulty in seasonal predictions is that given a particular state of ocean sea surface temperatures more than one atmospheric state is possible. Therefore, small changes in physical parameterizations in a General Circulation Model (GCM) can yield significantly different large-scale flows and model sensitivity to boundary forcing as shown in previous studies (e.g., Palmer and Mansfield 1986; Meehl and Albrecht 1991). From this fact, the claim can be made that a GCM containing improved sensitivity to boundary forcing offers the best chance for accurate climate predictions (Kumar et al. 1996).

Before implementation of a GCM, its accuracy in predicting seasonal variability should be investigated. This investigation uses climate simulations and hindcasts, which are compared to observations. In order to achieve an accurate comparison, a large enough sample size must be used to decrease internal variability and model noise. Because

1

seasonal atmospheric responses are sensitive to initial conditions, an ensemble of model

integrations is made with identical boundary forcings as done in Kumar et al. (1996).

Evaluating a GCM's ability is not straightforward; therefore only through averaging over

many cases of similar boundary forcing can the predictable signal be identified (e.g.

Kumar et al. 1996). Ensemble averaging acts to reduce the influence of random internal

variability, and the ensemble mean shows the region where the observed anomalies are

more likely to occur (Kumar and Hoerling 1995, 2000).

In this study, a 10-member ensemble of the NCEP operational climate model is

investigated in order to determine skill in predicting winter (JFM) mean temperature and

precipitation patterns over the U.S. The goal of the study is to examine the model's

ability to predict seasonal patterns, not to investigate the model's physical

parameterization or to suggest possible changes. Comparisons are made for seasonal

means, extreme events, and as a function of ENSO and AO phase. ENSO and AO are

two of the leading patterns of natural climate variability. It has been argued that skill in

climate forecasting will come from an ability to forecast these patterns (Higgins et al.

2000). The AO was used in this study and not the North Atlantic Oscillation (NAO),

because Thompson and Wallace (1998) showed that the AO accounts for a substantially

larger fraction of the variance in Northern Hemisphere surface air temperature than NAO.

Because seasonal prediction is viewed as a boundary forcing problem instead of

an initial value problem, atmospheric initial conditions are largely ignored. Though not

proven, the possibility exists that atmospheric initial conditions can have impacts on

seasonal prediction. In this new seasonal prediction system, atmospheric initial

2

conditions are included. The initial conditions include both high and low frequency components. Examples of the low frequency modes are the Pacific North America (PNA), NAO, and AO. If the model is capable of predicting or maintaining low frequency modes then atmospheric initial conditions may be of importance (Kanamitsu et al., in press). The model's ability to predict these low frequency modes is another reason AO patterns are examined in this study.

2. MODEL AND OBSERVATIONAL DATA

a. Model Data

In our study, we have utilized the 21-year hindcasts of the NCEP operational climate prediction GCM runs. The model is a coupled ocean-atmospheric model with 10 ensemble members for the 1979-1999 period. The lead time is two months, and initial conditions, both atmospheric and oceanic, are updated yearly. For the 10 member ensemble used in this study, the corresponding initial conditions are chosen from the first 5 days of the month at 12 hour intervals. Because JFM is the season and the lead time is two months, the initial conditions are from November 1-5 at 00Z and 12Z. The model has T62L28 resolution with output on a 2.5° x 2.5° grid. The boundary condition over the oceans is provided from the NCEP global weekly sea-surface temperatures (SSTs) analysis. A more detailed description of the model is given in the appendix.

b. Observations

NOAA/NCEP Climate Prediction Center (CPC) provided the observations used in our study. The data for mean temperature and precipitation are observed station data from 1979-1999 over the U.S. placed on 1.0° x 1.0° grid.

In order to investigate the model's ability to predict patterns associated with ENSO and AO, classifications of ENSO and AO events were needed. The ENSO classification is subjective and based on the pattern and magnitude of the SSTs in the equatorial Pacific. Some of the processes involved are described in Rasmusson and Carpenter (1983) and Ropelewski and Halpert (1987) for warm episodes and Ropelewski and Halpert (1989) for cold episodes. Table 1 shows the classification of years into ENSO warm, cold, or neutral events.

The AO classification is also provided by CPC. It is based on the Thompson-Wallace methodology (Thompson and Wallace 2000). The indices classified by CPC and Thompson-Wallace methodology have a 0.99 correlation, so they are virtually identical. The AO indices were normalized as in equation (1) (Wilks 1995).

$$\text{Normalized AO} = \frac{x - \bar{x}}{s} \qquad (1)$$

where x is each individual seasonal index, $\bar{x}$ is the mean from 1979-1999, and s is the standard deviation of all x. Normalized values greater than 0.5 were considered positive AO events, and normalized values less than –0.5 are considered negative AO events. Figure 1 shows the yearly values of normalized AO index, and Table 2 lists the AO classification.

Table 1. Yearly classifications of ENSO warm, neutral, and cold events from JFM 1979-1999 based on the pattern and magnitude of SST anomalies in the tropical Pacific. Classifications of ENSO events are by NOAA/NCEP Climate Prediction Center.

Warm Events	Neutral Events	Cold Events
1983	1979-1982	1989
1987	1984-1986	1999
1992	1988	
1998	1990-1991	
	1993-1997	
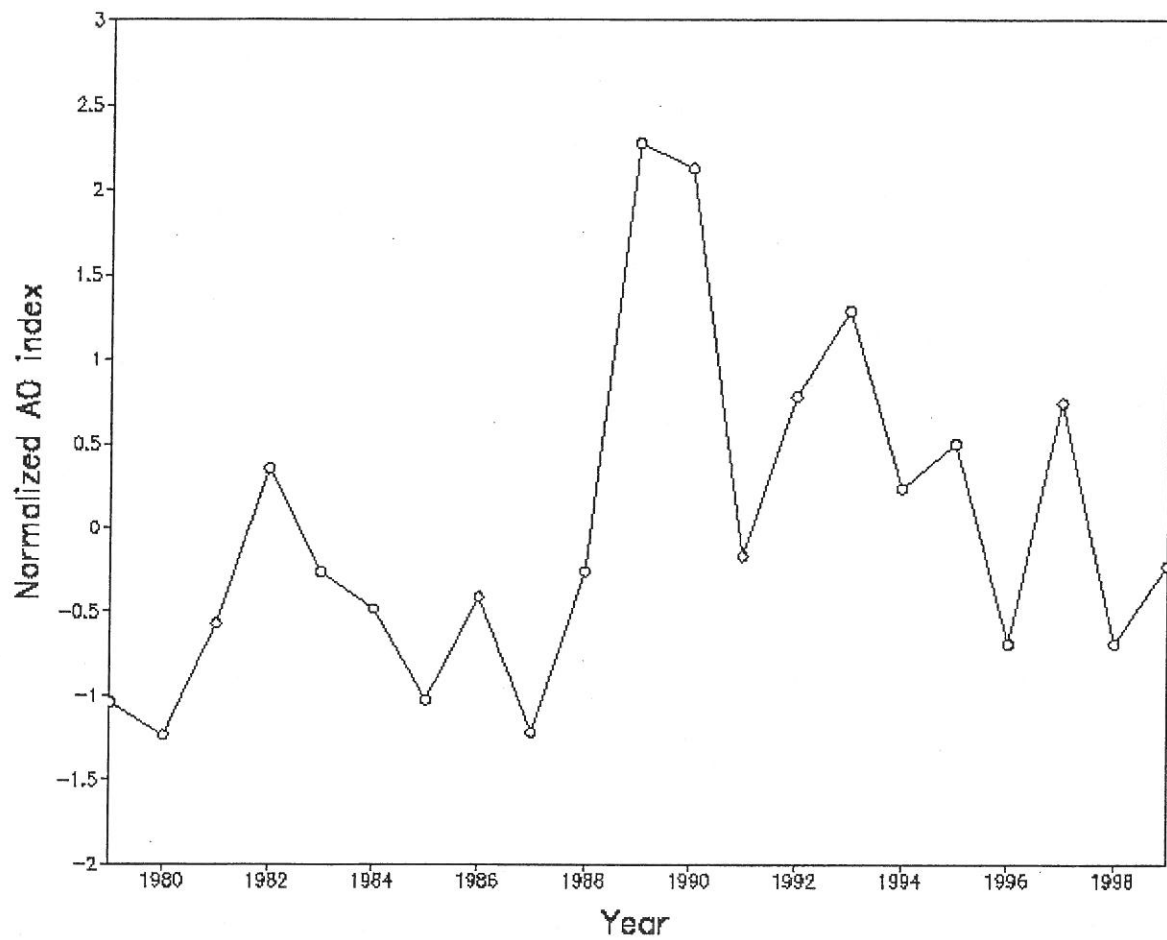
Figure 1. Yearly JFM values of normalized AO index from 1979-1999. Using equation 1, AO values were normalized. Normalized values greater than 0.5 are considered positive events and normalized values less than −0.5 are considered negative events. There are 5 positive events, 7 neutral events, and 9 negative events.

Table 2. Yearly JFM classifications of AO positive, negative, and neutral events from 1979-1999. Seasonal AO indices were provided by NOAA/NCEP Climate Prediction Center. AO values were normalized using equation 1. Normalized values greater than 0.5 were considered positive events, and normalized values less than −0.5 were considered negative events.

Positive Events	Neutral Events	Negative Events
1989	1982-1984	1979
1990	1986	1980
1992	1988	1981
1993	1991	1985
1997	1994-1995	1987
	1999	1996
		1998

3. DATA PROCEDURE

The model outputs analyzed are daily maximum and minimum temperature and daily precipitation rate. Daily mean temperatures are obtained by combining the maximum and minimum temperatures. For both mean temperature and precipitation the ensemble mean is obtained by averaging the 10 ensemble members. The differences in mean temperature and precipitation among ensemble members are small, meaning the internal variance (i.e. ensemble spread) of the model is small, and therefore the differences between the model and observations are caused by external variability (i.e. response to different boundary forcing). Once the model ensemble data are placed in a single continuous daily record from 1979-1999, comparisons to observations are made after the forecast data and observations have been interpolated to the same resolution (0.25° x 0.25°).

For extreme events, the model and observed data are also ranked from high to low. The top and bottom 1%, 5%, and 10% were compared for mean temperature but only the top 1%, 5%, and 10% for precipitation (precipitation is not normally distributed, and the most common occurrence is no precipitation). For ENSO and AO comparisons, model and observed averages were computed for all years that fell into a particular category (i.e., all ENSO warm events were averaged). Model ensemble anomalies are obtained by comparing seasonal forecasts to model climatology from 1979-1999, and

observed seasonal anomalies are obtained by comparing seasonal observations to observed climatology from 1979-1999. Defining anomalies in this fashion eliminates any inherent biases in the model or observed data.

Other statistical measures are used, such as root-mean-square error (RMSE), anomaly correlation (AC), and RMS skill score (SS). The equations used are standard for verifying data sets and can be found in Wilks (1995). Like the ENSO and AO, model forecasts are compared to model climatology and seasonal observations are compared to observed climatology.

The equations are:

$$\text{RMSE} = \sqrt{\frac{1}{M}\sum_{m=1}^{M}(y_m - o_m)^2} \qquad (2)$$

where M = 21, y = individual seasonal forecasts of variable y, o = individual seasonal observations of variable y, and m = each individual event of the variable y,

$$\text{AC} = \frac{\sum_{m=1}^{M}[(y_m - C_m)(o_m - C_m)]}{[\sum_{m=1}^{M}(y_m - C_m)^2 \sum_{m=1}^{M}(o_m - C_m)^2]^{1/2}} \qquad (3)$$

where C_m = the climatological value of the variable y_m in $(y_m - C_m)$ and o_m $(o_m - C_m)$,

$$\text{SS} = 100 \cdot (1 - \frac{RMSE_{fore}}{RMSE_{ref}}) \qquad (4)$$

10

4. RESULTS

We begin our evaluation of the model forecast by comparing the climatology of the model to that of observations over the 21-year period. The model (Fig. 2) has a cold bias throughout the Northeast, the Mid-Atlantic, the Great Lakes states, and in the southwest along the Rocky Mountains. The biases are greater than 2°C per day throughout much of New England, as well as Ohio and Michigan. Small regions of warm bias are located in the northern Great Plains and Florida.

The regions of largest bias correspond well to the regions of largest RMSE (Fig. 3). Because RMSE include biases in the mean and errors in the variance or spread, the strong similarities between Figs. 2 and 3 indicate that these biases are fairly persistent and not skewed by a few large errors.

The model precipitation rate (Fig. 4) is higher than observations across most of the U.S. Only along the Pacific coast and along the northern Gulf is the model not positively biased. The bias in most places is less than 2 mm/day except in the Pacific Northwest, where biases are greater than 2 mm/day and as much as 4 mm/day. The precipitation rate is highest in the Pacific Northwest for the winter season (Fig. 6). The two areas in the mean that show no positive bias (along the Pacific coast and northern Gulf) have large RMSE errors (Fig. 5). The large RMSE are most likely due to errors in the spread of the data and may be a result of errors in extreme events. Though the model

11
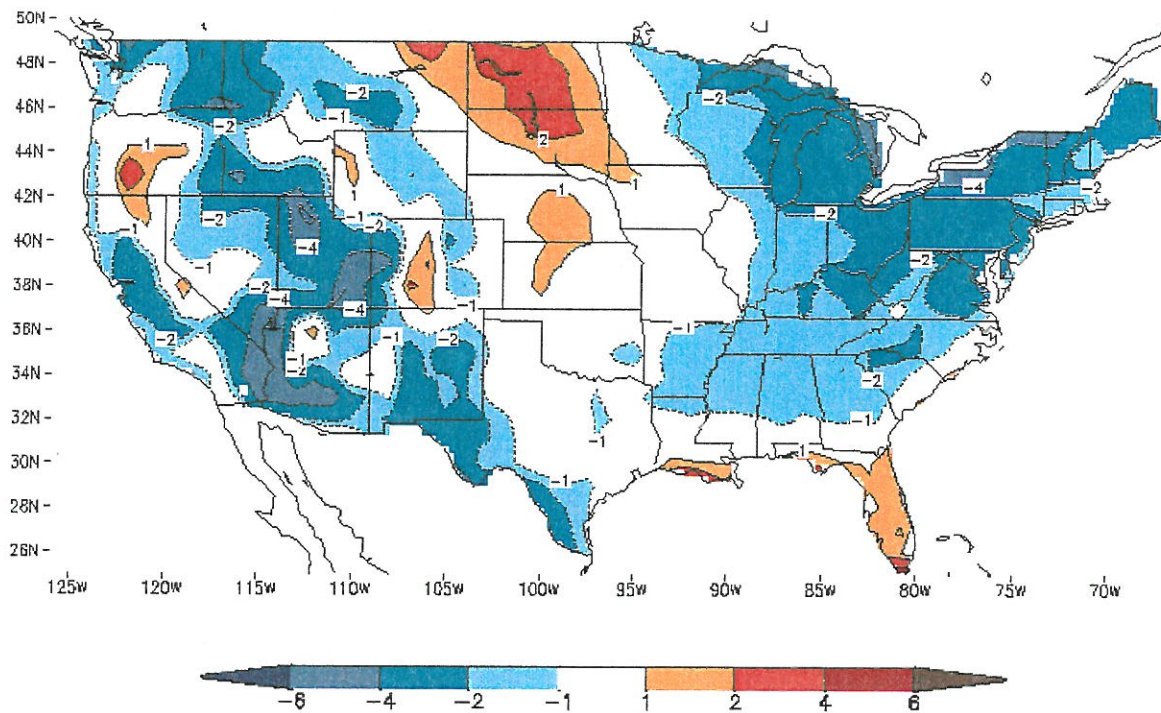
Figure 2. Average daily mean temperature bias (ºC) of model ensemble compared to observations for 21 year record. Positive regions are outlined with solid lines and negative regions outlined with dashed lines. Negative biases are located in the Northeast, Great Lakes, and Southwest, while a positive bias is located in the northern Great Plains.
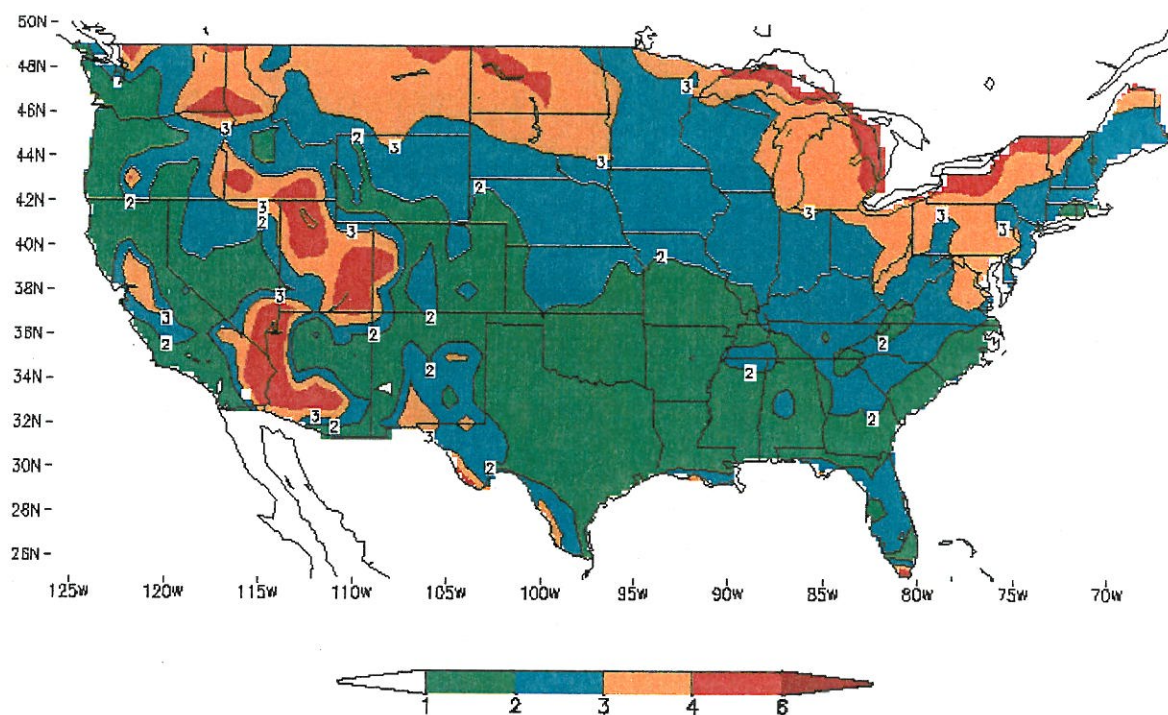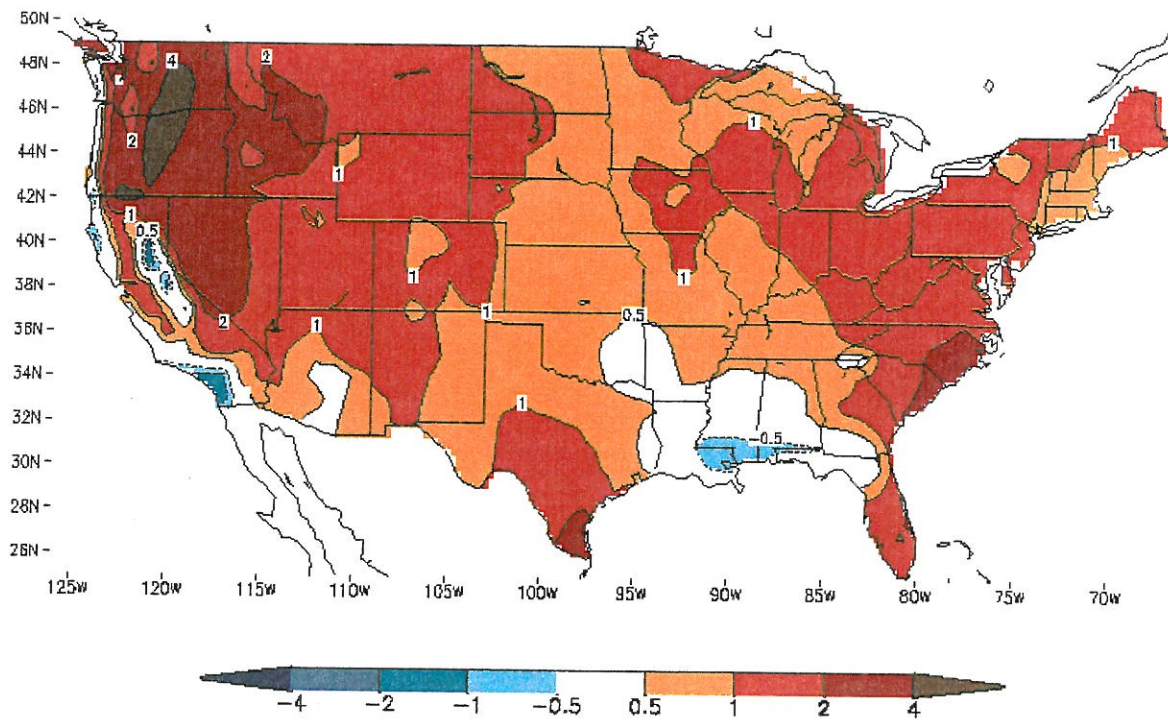
Figure 3. Seasonal mean temperature (°C) RMSE of model ensemble compared to observations for 21 year record. The areas containing the largest errors correspond match the regions with the largest biases in the mean.

Figure 4. Average daily precipitation rate bias (mm/day) of model ensemble compared to observations for 21 year record. Positive regions are outlined with solid lines and negative regions outlined with dashed lines. Positive biases are present throughout the country except along the northern Gulf and Pacific coasts.
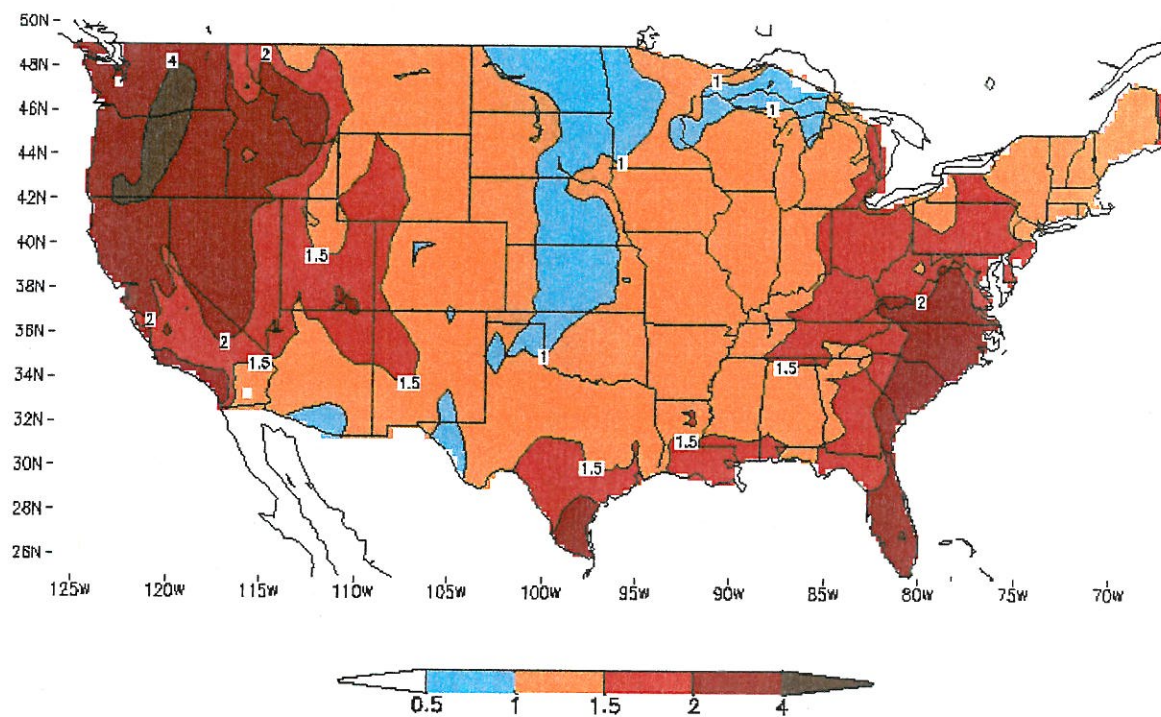
Figure 5. Seasonal daily precipitation rate (mm/day) RMSE of model ensemble compared to observations for 21 year record. Errors are small (less than 1.5 mm/day) for most of the country except in the Pacific Northwest and the Mid-Atlantic. Areas in the mean that show no positive biases have large RMSE.
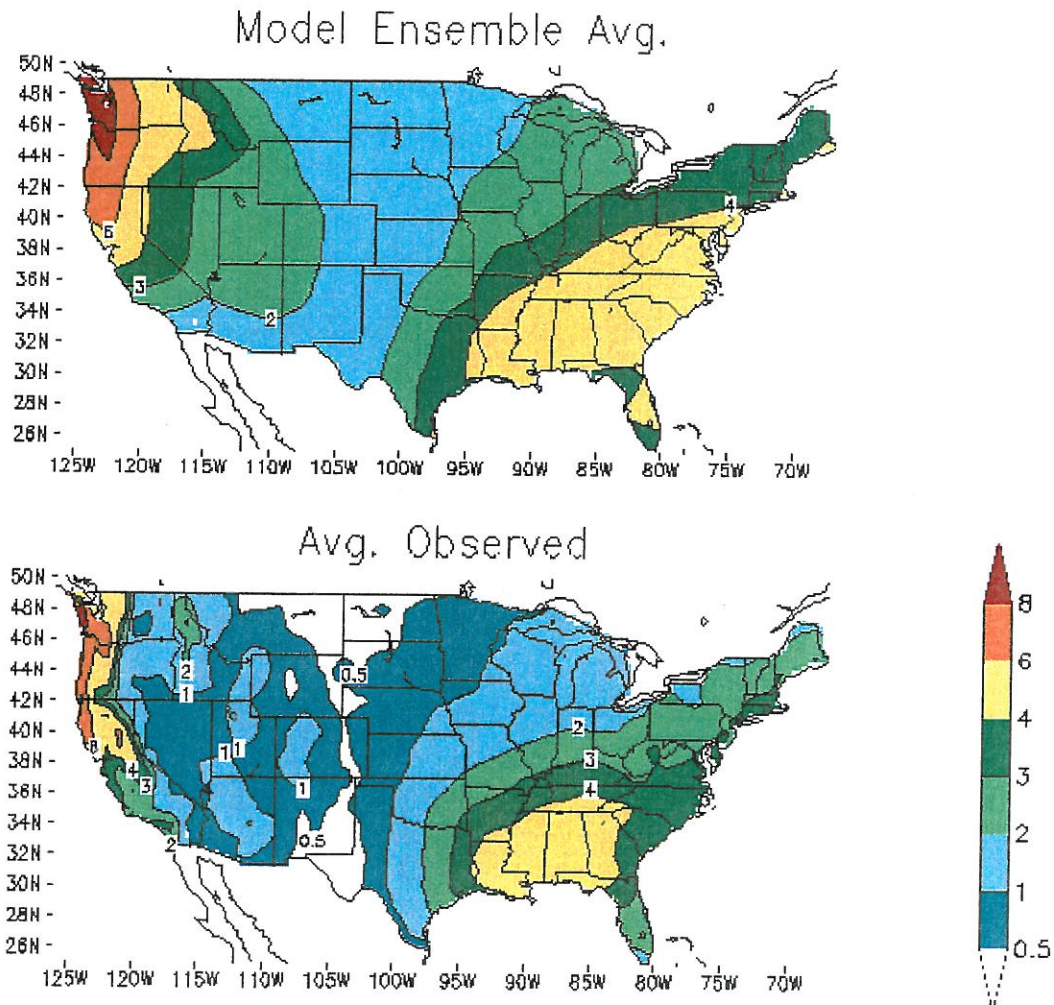
Figure 6. Average daily precipitation rate (mm/day) of model ensemble and observations for 21 year record. Though the model produces higher precipitation rates almost everywhere, the spread of precipitation and which regions receive the most and least precipitation is represented well.

has a positive bias, it does well in representing which regions receive the largest and smallest amounts of precipitation during the winter season (Fig. 6).

The model has difficulty producing extreme events (i.e. events for the 1st, 5th, 10th, 90th, 95th, and 99th percentiles). The problem is expected; because climate models are known to have less variance in their spread, as a result the amplitude of the ensemble forecasts tends to be less than observations. The highest model daily temperatures at the 90th, 95th, and 99th percentiles (Fig. 7) are lower than observations everywhere by at least 2°C and as much as 8°C. However, at the cold extremes the model temperatures are higher than observations by at least 2°C and as much as 10°C for most of the country (Fig. 8). The differences between the model warm and cold extreme events and observed values are opposite but not always of similar magnitudes. For example, in the warm bias region over the northern Great Plains (Fig. 2) for the warm extreme events (Fig. 7) the model has negative values ranging from -2°C to -6°C, while for the cold extreme events (Fig. 8) the model has positive values greater than 6°C throughout. A similar but opposite pattern exists for the cold bias in the Northeast. The differences in producing extreme cold or warm events may help increase the magnitude of the cold and warm biases in the ensemble mean, but since the biases are both extremes they indicate the biases are consistent throughout. The analysis of extreme events and RMSE indicate that biases in the mean may be persistent throughout the spread.

For extreme precipitation events (Fig. 9), the model does well at the 90th percentile, showing only small biases, but by the 99th percentile the model has a negative bias across the entire eastern half of the U.S. and the Pacific coast by as much as 12
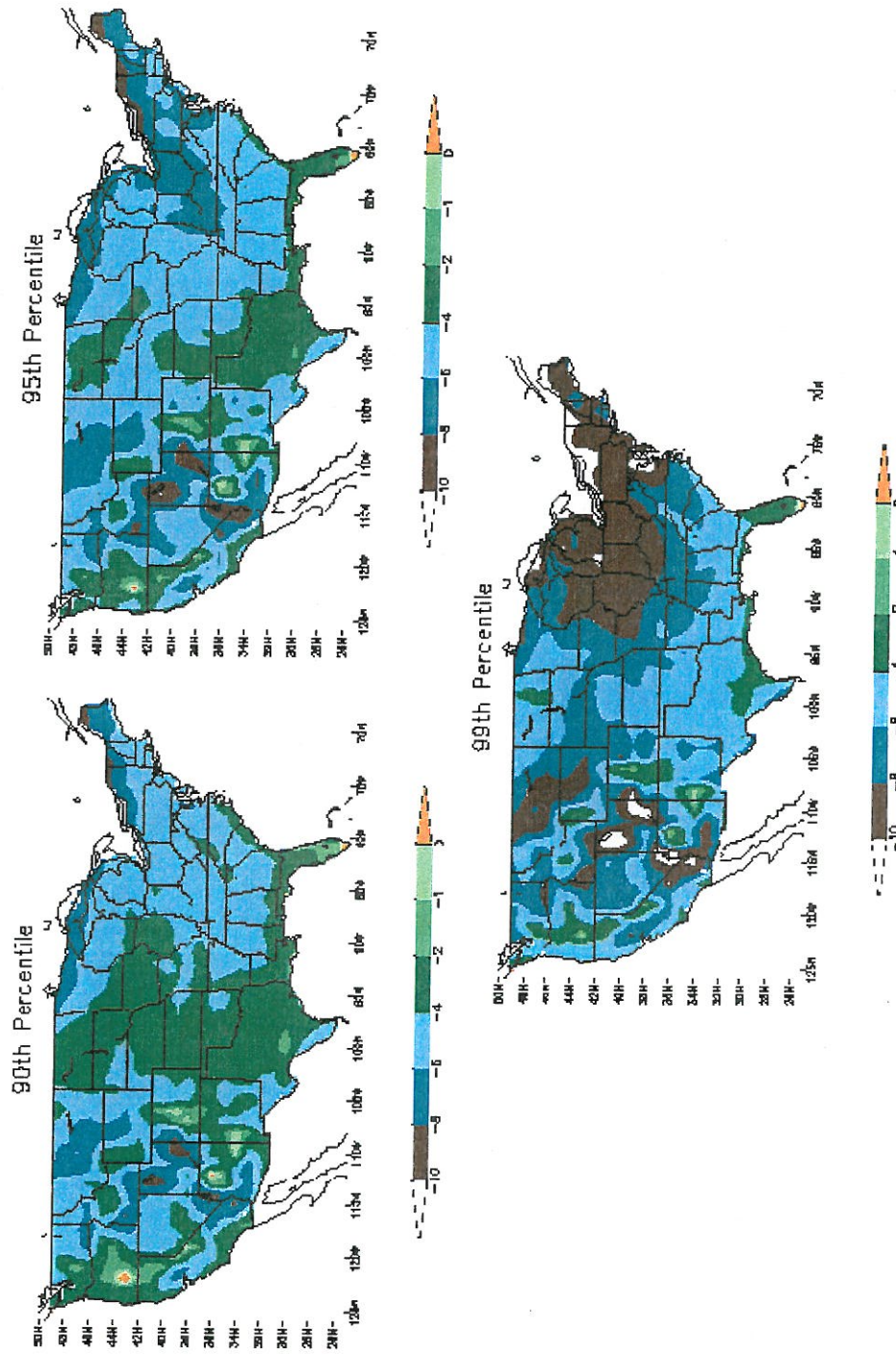
17

Figure 7. Daily mean temperature bias (°C) of model ensemble at the 90th, 95th, and 99th percentiles. Cold biases (model – obs. < 0) are present throughout the entire country at all three percentiles.
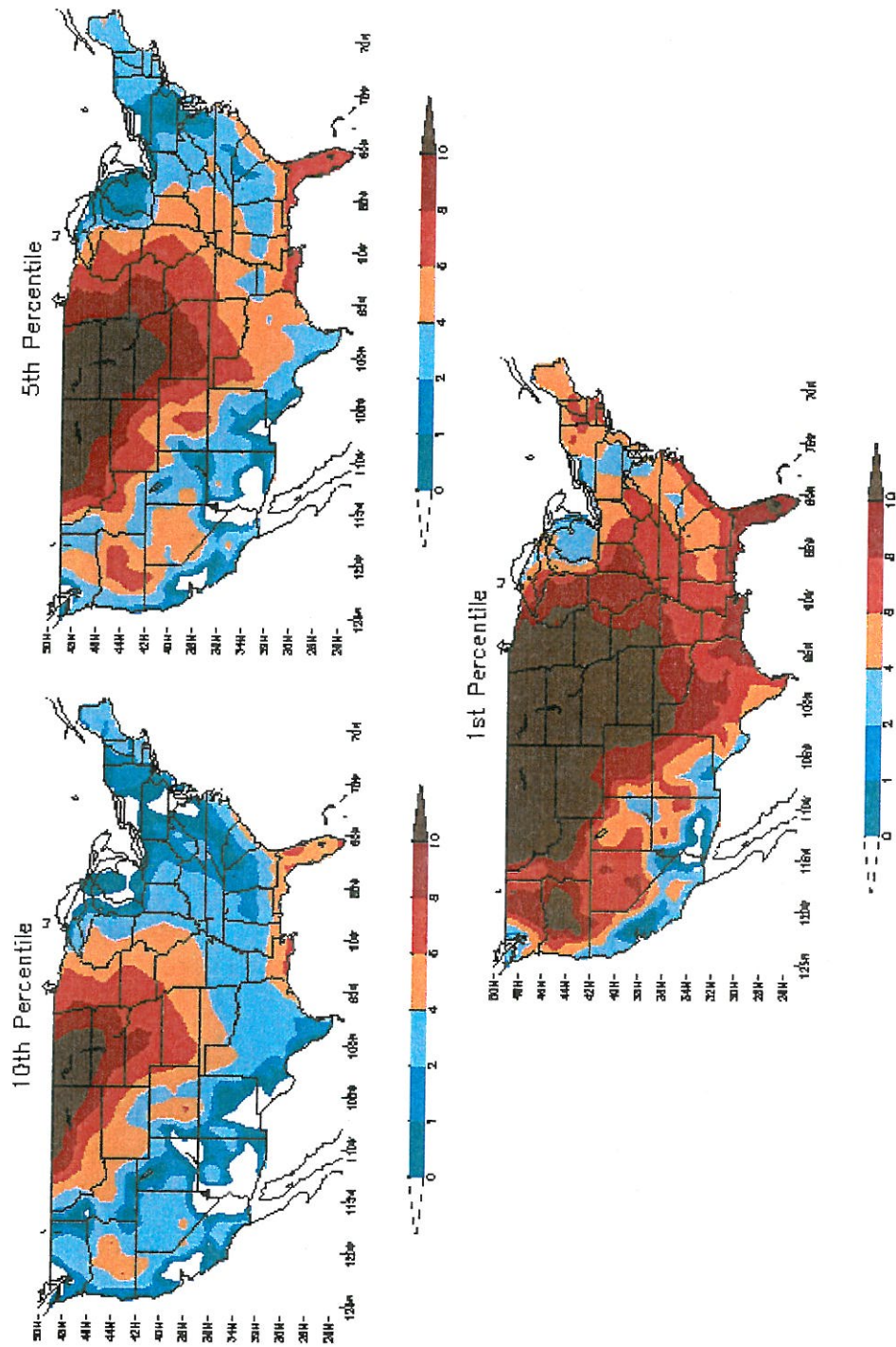
Figure 8. Daily mean temperature bias (°C) of model ensemble at the 10th, 5th, and 1st percentiles. Warm biases (model – obs. > 0) are present throughout the entire country at all three percentiles.
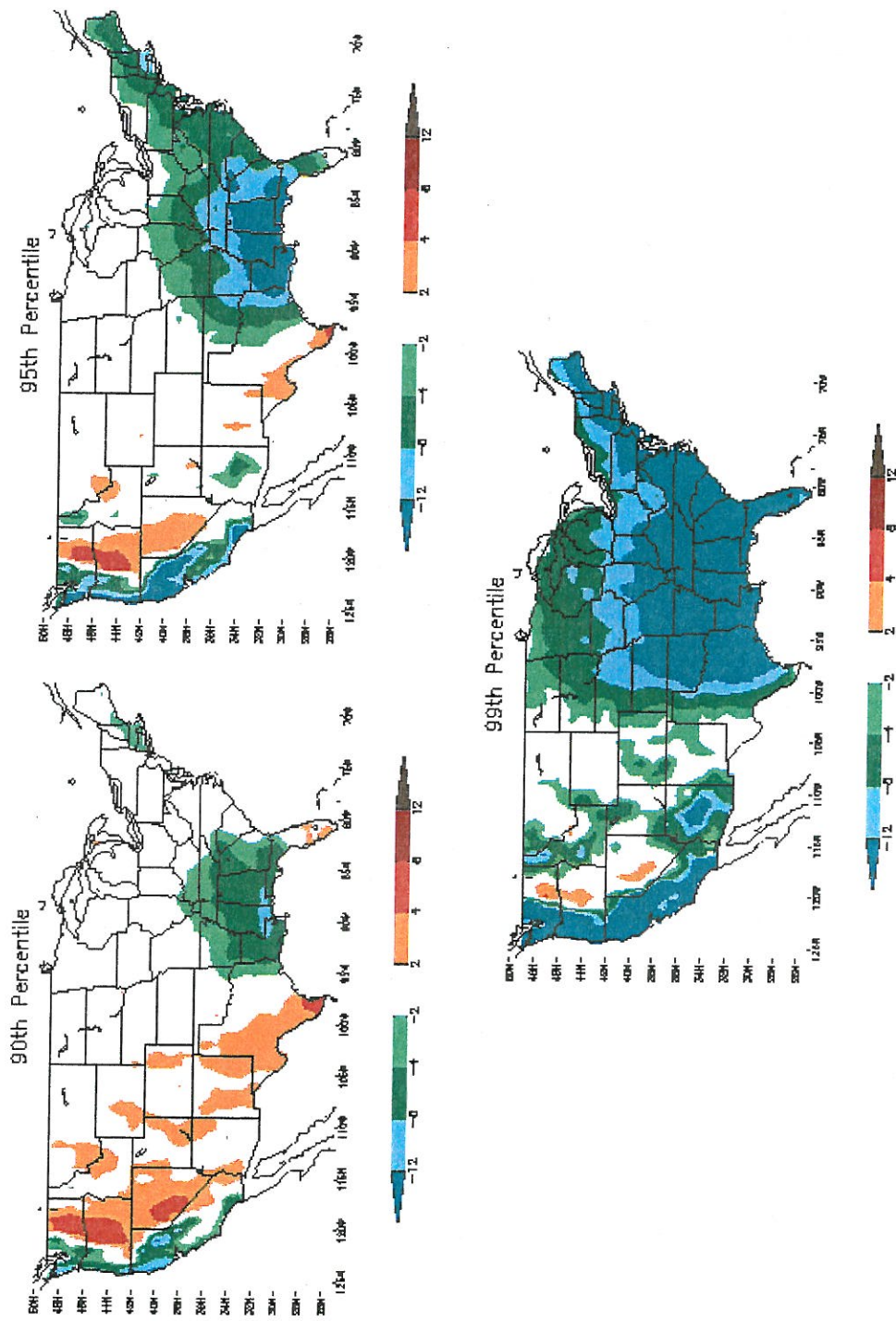
Figure 9. Daily precipitation rate (mm/day) of model ensemble at the 90th, 95th, and 99th percentiles. Negative biases (model − obs. < 0) are present along the northern Gulf and Pacific coasts at all three

20

mm/day. However, the two regions that show strong negative biases at all three percentiles are along the northern Gulf Coast and the Pacific Coast. The lack of extreme events in these regions helps explain the large RMSE in the regions, and why no positive bias exists in the mean pattern.

As stated earlier, for a GCM to be useful, it must be able to predict major climate variations like those associated with ENSO. The period 1979-1999 contains four major warm events and two major cold events (Table 1).

Average seasonal anomalies for mean temperature for the warm events are shown (Fig. 10). Observations show the traditional El Nino pattern, which is warm temperatures along the northern half of the country and cool temperatures in Florida and the Desert Southwest. The model (Fig. 10) depicts some warming in the Northeast and Great Lakes, but the warm anomalies are 4-8 times smaller than observations. The model actually shows cold conditions in the Pacific Northwest and failed to produce the cold anomalies in Florida and the Southwest. The modeled precipitation pattern also shows significant bias (Fig. 11). In regions where positive anomalies are present in observations (e.g., California and the deep south) the model has negative anomalies.

Individual analysis of the 1992 and 1998 warm ENSO events are shown in Figs. 12-15. Model temperature anomalies for the 1992 event are negative and completely opposite of the observed positive anomalies (Fig.12). The precipitation rate anomalies for the 1992 event correlate well with observations (Fig. 13). The model produces similar positive anomalies along the Gulf Coast and similar negative anomalies in the Mid-Atlantic, Northeast, and Pacific Northwest. For the 1998 warm event, the model and
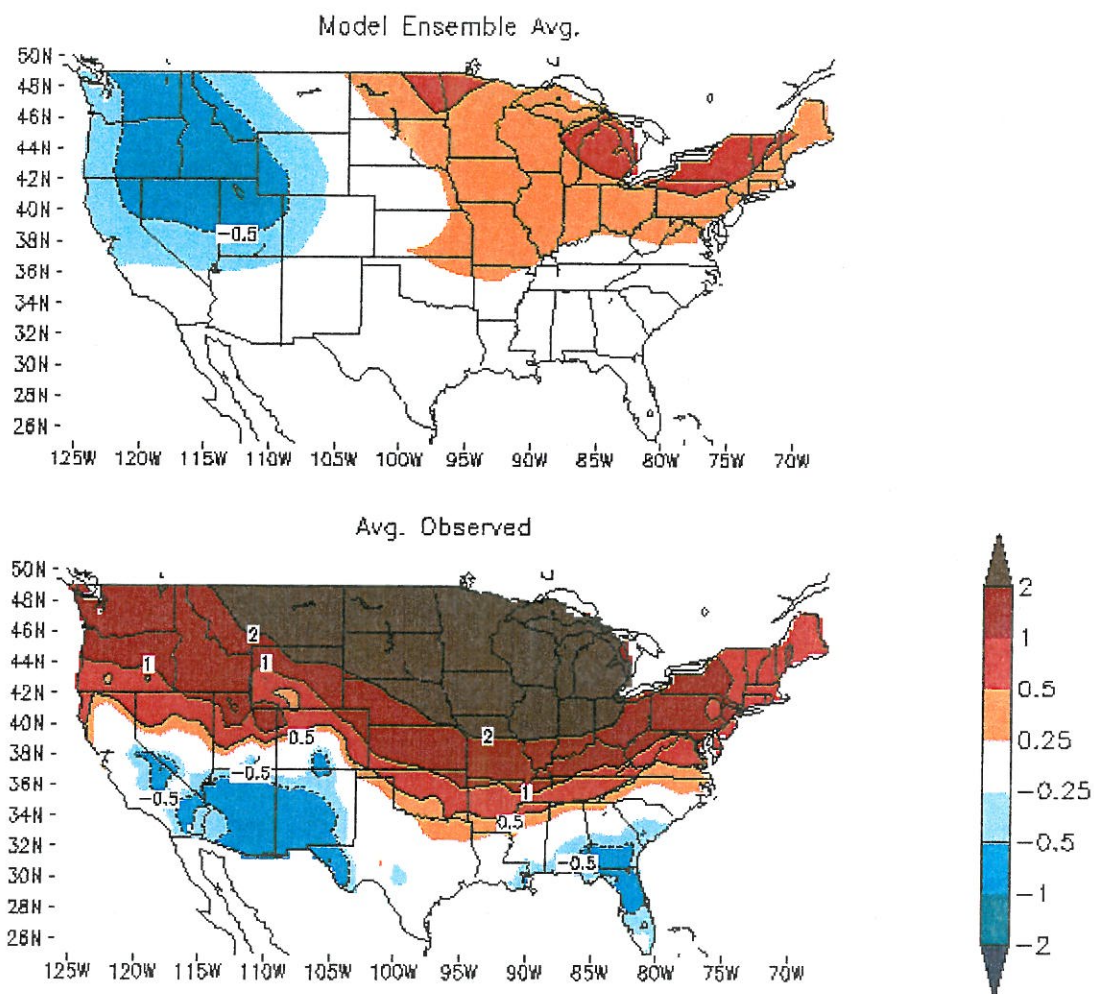
21

Figure 10. Average daily mean temperature anomalies (ºC) during ENSO warm events for model ensemble and observations.   Positive regions are outlined with solid lines and negative regions outlined with dashed lines. The model shows warm anomalies in the Northeast and Great Lakes region, but the magnitudes are much smaller.
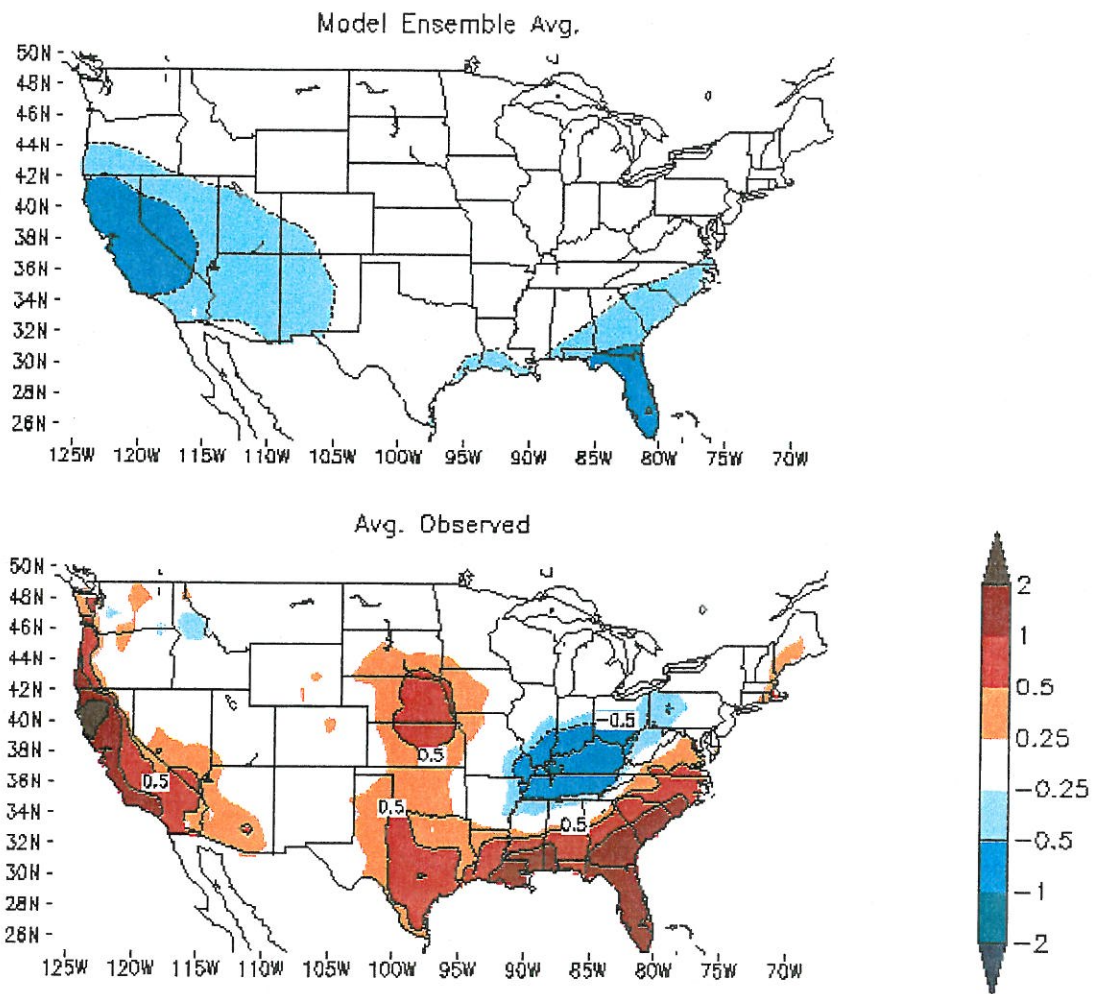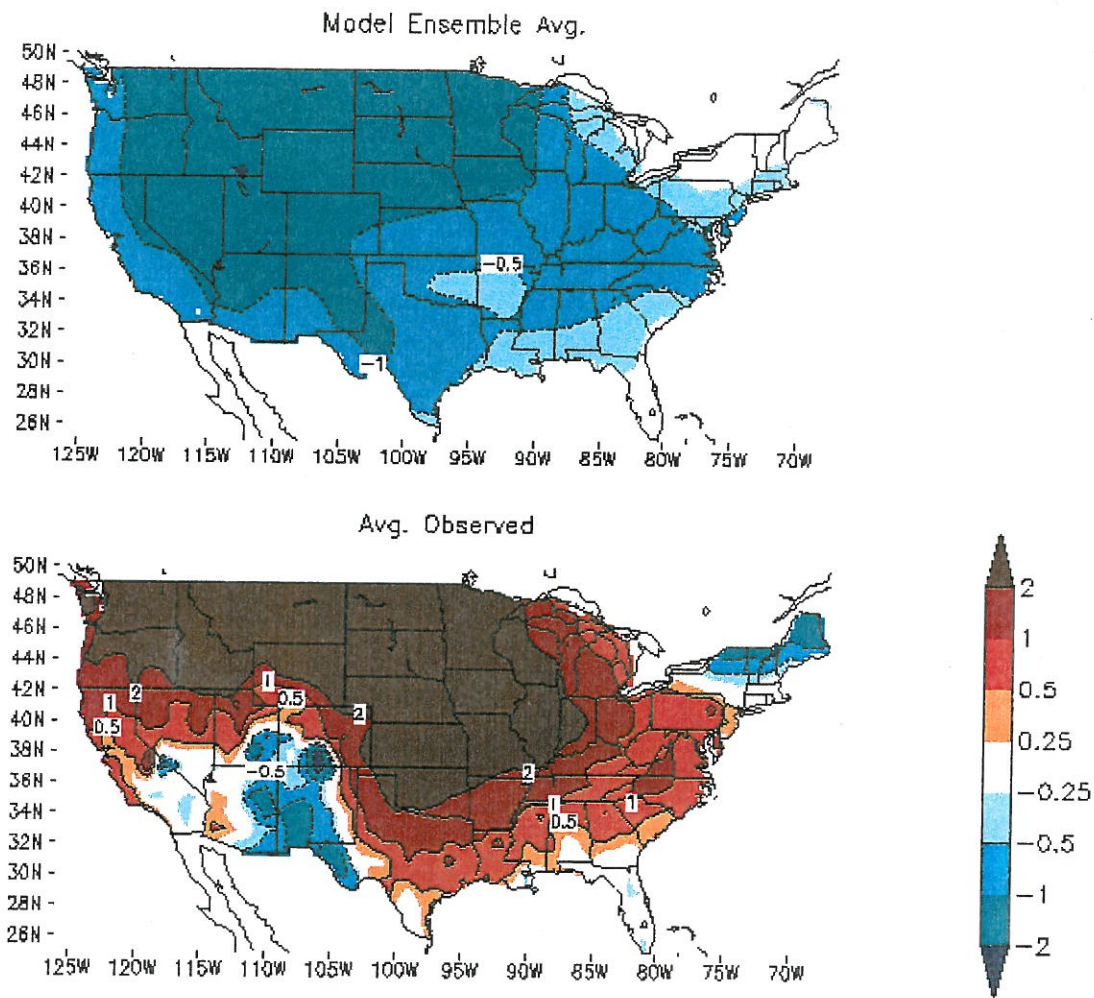
Figure 11. Average daily precipitation rate anomalies (mm/day) during ENSO warm events for model ensemble and observations. Positive regions are outlined with solid lines and negative regions outlined with dashed lines. The model fails to produce the positive anomalies in the Southeast.

Figure 12. Average daily mean temperature anomalies (ºC) during the 1992 ENSO warm event for model ensemble and observations. Positive regions are outlined with solid lines and negative regions outlined with dashed lines. The model shows negative anomalies everywhere which is the opposite anomaly pattern shown in the observations.
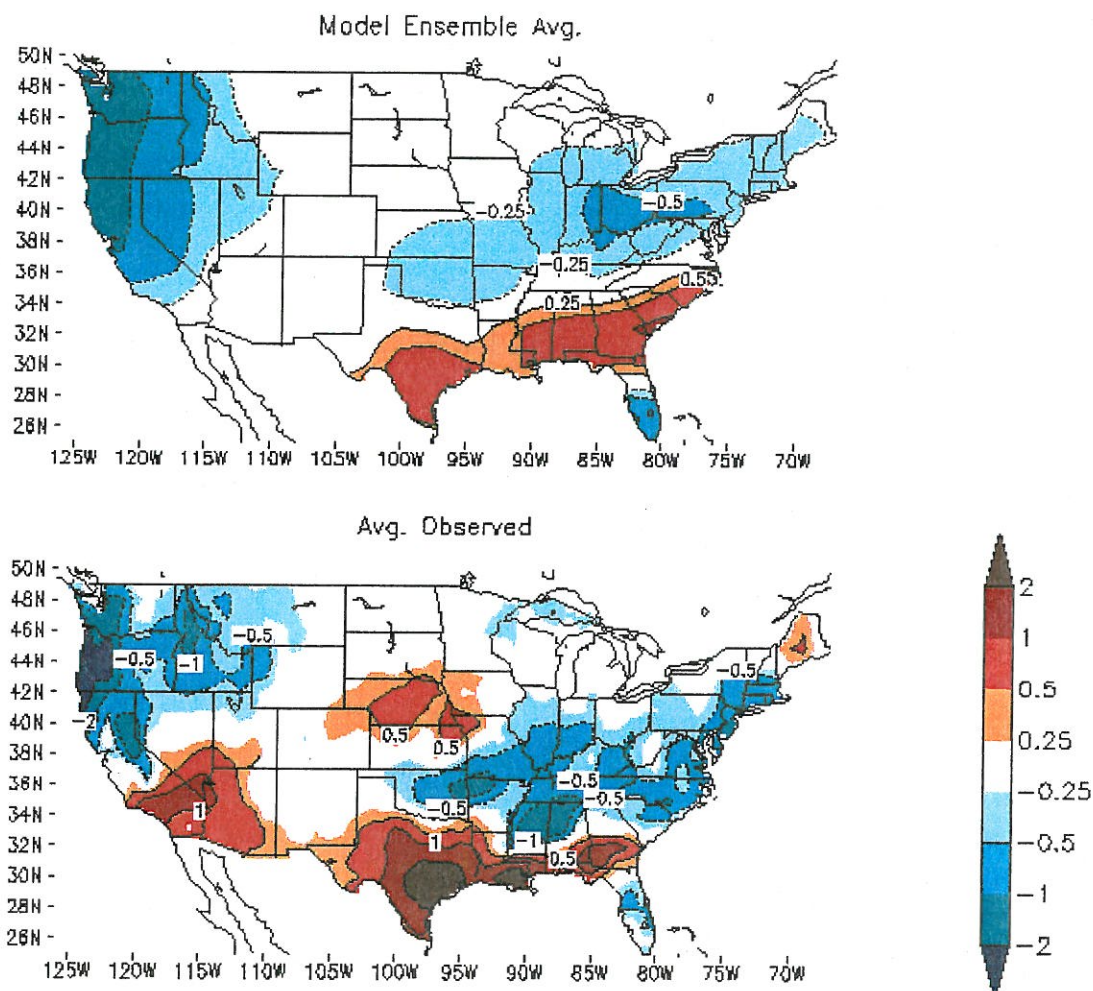
Figure 13. Average daily precipitation rate anomalies (mm/day) during the 1992 ENSO warm event for model ensemble and observations. Positive regions are outlined with solid lines and negative regions outlined with dashed lines. The model produces similar positive anomalies along the Gulf Coast and similar negative anomalies in the Mid-Atlantic, Northeast, and Pacific Northwest.
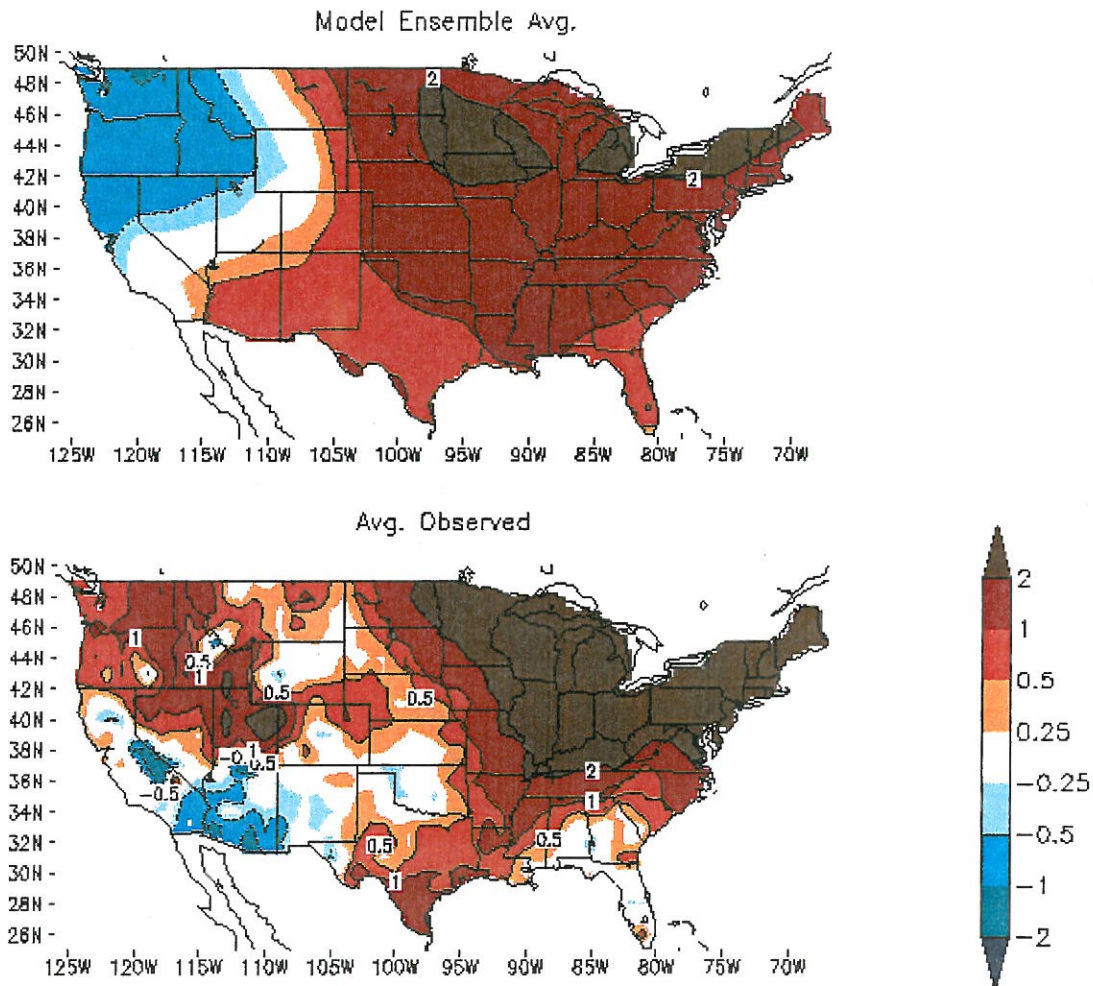
Figure 14. Average daily mean temperature anomalies (°C) during the 1998 ENSO warm event for model ensemble and observations. Positive regions are outlined with solid lines and negative regions outlined with dashed lines. The model and observed patterns show warm anomalies through the eastern half of the country. The only opposite anomalies are in the Pacific Northwest and Desert Southwest.
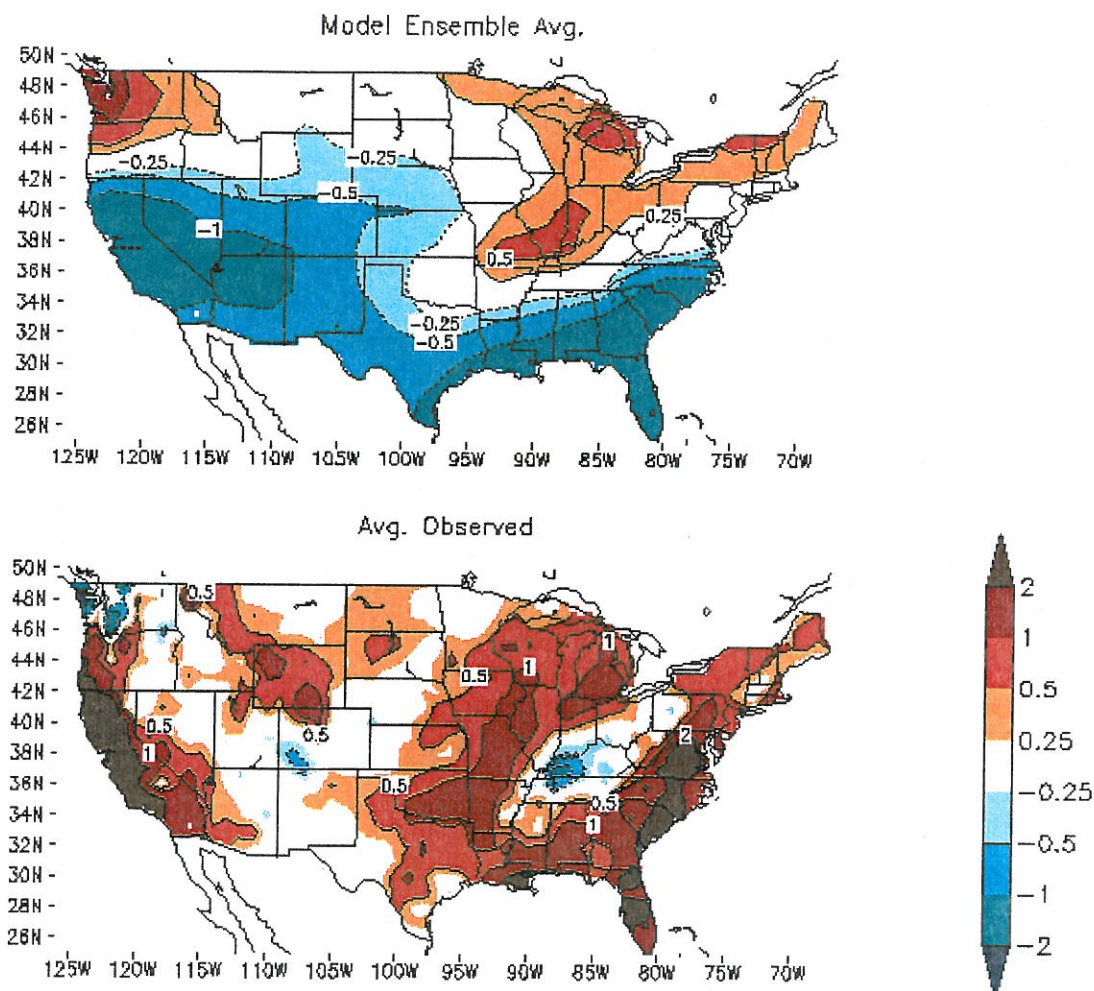
Figure 15. Average daily precipitation rate anomalies (mm/day) during the 1998 ENSO warm event for model ensemble and observations. Positive regions are outlined with solid lines and negative regions outlined with dashed lines. The model fails to produce the positive anomalies along the east coast and California and fails to produce the negative anomalies in the Pacific NW and Ohio River valley.
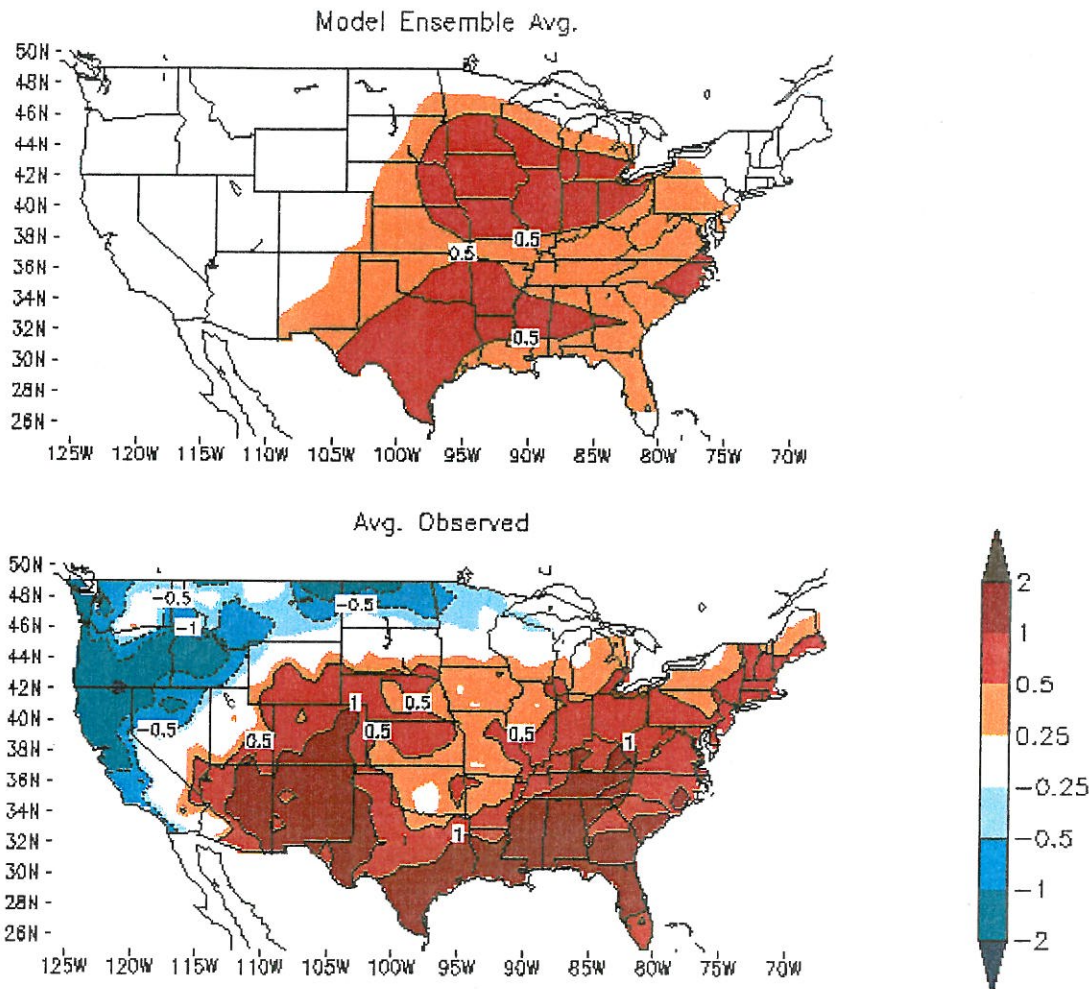
27

Figure 16. Average daily mean temperature anomalies (°C) during ENSO cold events for model ensemble and observations. Positive regions are outlined with solid lines and negative regions outlined with dashed lines. The positive anomalies for the eastern half of the country are represented well, but the negative anomalies along the west coast and extreme northern Great Plains are not produced.
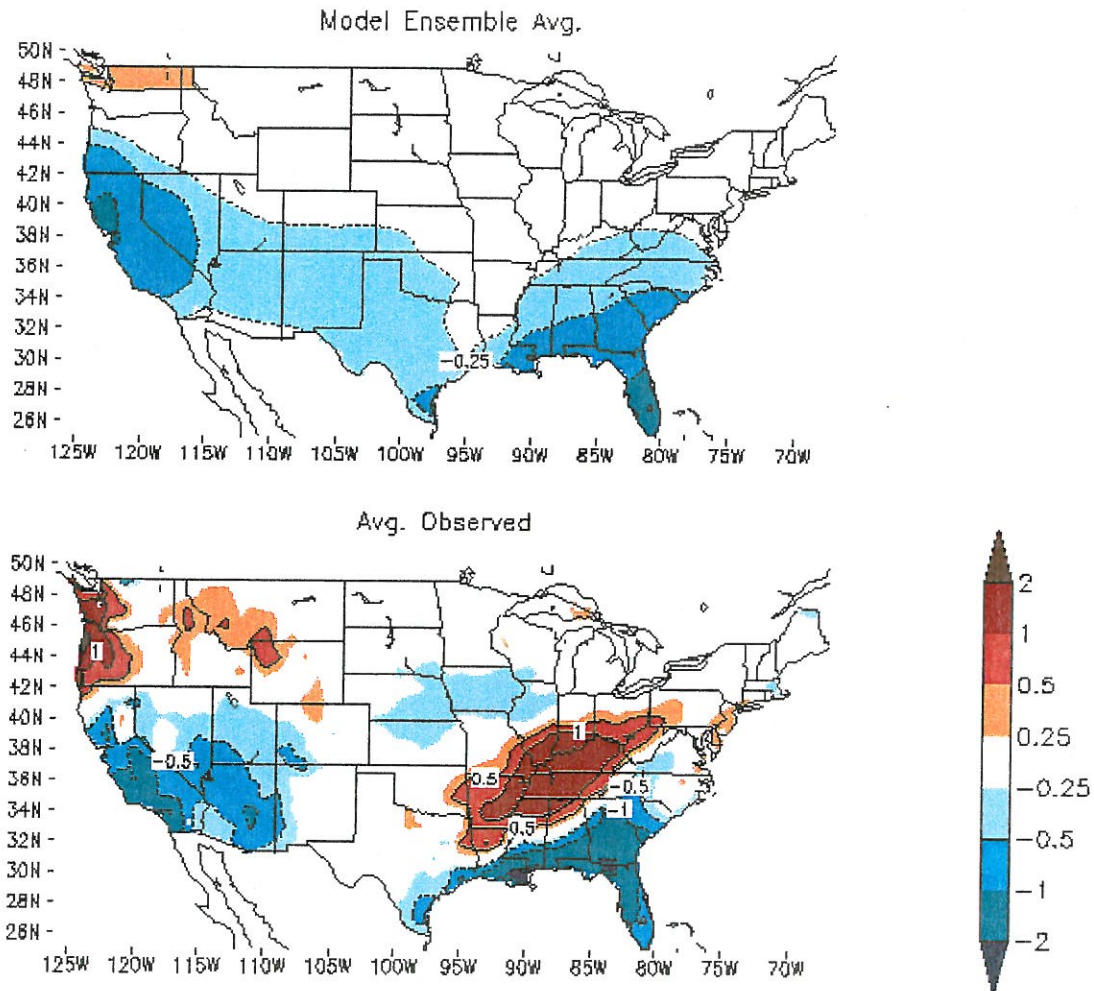
Figure 17. Average daily precipitation rate anomalies (mm/day) during ENSO cold events for model ensemble and observations. Positive regions are outlined with solid lines and negative regions outlined with dashed lines. Negative anomalies are produced in the Deep South and Florida, but the positive anomalies in the Ohio River valley are not represented in the model.

observed patterns show warm anomalies through the eastern half of the country. The only opposite anomalies are in the Pacific Northwest and Desert Southwest (Fig. 14), but for precipitation the model fails to produce the positive anomalies along the east coast and California and fails to produce the negative anomalies in the Pacific NW and Ohio River valley (Fig. 15).

Cold ENSO temperature anomalies (Fig. 16) correlate better with observations than those of warm events. Similar positive anomalies appear from the East Coast to the Central Plains, although the magnitudes are smaller for the model. Observations show negative anomalies along the Pacific Coast and the Northwest, and the model shows no significant patterns (i.e. anomalies greater than $|0.25|$) in these regions. In fact, no regions of negative anomalies are present. For precipitation (Fig. 17), the model produces negative anomalies similar to observations in the Deep South, Florida, California, and the desert southwest, but it fails to produce the positive anomalies along the Ohio and Mississippi River valleys.

The results of the ENSO analysis indicate that the model's ability to produce ENSO patterns, on average, is limited. But the analysis of the individual events suggests that the model may have the ability to produce similar anomaly patterns of certain variables for an individual ENSO event. Model sensitivity to the SST boundary forcing may be responsible for the errors.

Like ENSO, the AO is a major controller of wintertime climate patterns (Thompson and Wallace 1998; Higgins et al. 2000). In the 21 years of record used in ourstudy, five positive and seven negative AO events occurred (Table 2). Temperature

and precipitation anomalies associated with AO positive events are shown in Figs. 18 and 19. For temperature (Fig. 18), the traditional observation pattern of warm temperatures throughout the eastern half of the U.S. is not found in the model average. In fact, the model produces negative anomalies over most of the country. For precipitation (Fig. 19), only two regions have significant patterns in observations; negative anomalies along the northern California coast and positive anomalies in the Mississippi River valley from eastern Texas to Kentucky. Negative anomalies are present in the Pacific Northwest instead of California, and a small positive region shifted to the Deep South.

The model AO negative anomalies for temperature (Fig. 20) fails completely in producing the cold anomalies throughout the majority of the U.S. For precipitation (Fig. 21), the model again shows no ability to produce the anomalies associated with AO negative conditions. These results suggest an inability of the model to maintain low frequency atmospheric modes. The model's inability to produce the positive precipitation anomalies along the East Coast during AO negative events, which are representative of the higher number of winter storms along the coast, is particularly problematic.

Temporal anomaly correlations are calculated so similarities in anomaly patterns can be detected. This is a very important test for a GCM, because the model's role is to predict higher or lower values compared to average for the variable of interest. Using equation 3, AC was calculated on a seasonal basis. Correlations for seasonal temperature and precipitation (Figs. 22 and 23) are poor. Anomaly correlations are less than 0.5

everywhere. In fact, for precipitation many of the anomaly correlations are negative, indicating that model and observations show opposite anomaly patterns.

Using equation 4, RMS skill scores were computed. RMS skill scores show areas where the model forecast is superior in comparison to some reference value, such as climatology or persistence. The improvement is a percent improvement over the reference (e.g., a SS of 10 means the forecast is a 10% improvement over the reference). For our study, both climatology and persistence were used as reference values in computing the SS. SS, with climatology as the reference, for mean temperature (Fig. 24) shows almost no regions are present where the model is better than climatology, but because we are examining seasonal forecasts we expect seasonal differences to be small so persistence is probably the better comparison. In this case, the observed values from JFM of the previous year were used. For example, when computing the skill of the mean temperature forecast for 1980, the forecast was compared to mean temperature observations from 1979. Persistence was used as the reference to calculate SS for mean temperature (Fig. 25). This calculation shows the model outperforming persistence for the Central Plains and some other small regions in the country. SS for seasonal precipitation rate using persistence as the reference (Fig. 26) shows an improvement in California and in the northern Gulf states. RMS skill scores for precipitation using climatology were calculated but showed no regions where the model outperformed climatology.
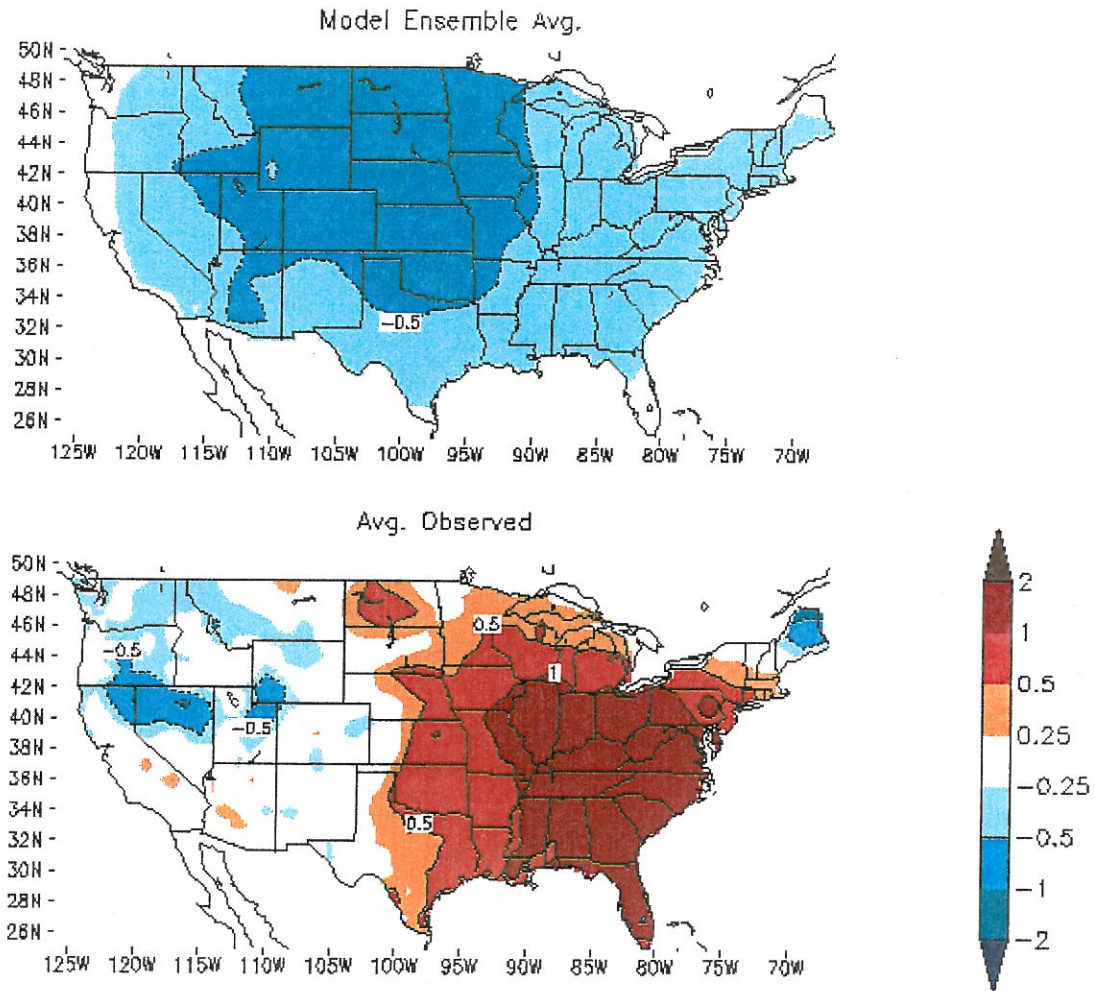
Figure 18. Average daily mean temperature anomalies (°C) during AO positive events for model ensemble and observations. Positive regions are outlined with solid lines and negative regions outlined with dashed lines. The model fails to produce the positive anomalies that occur in the observations.
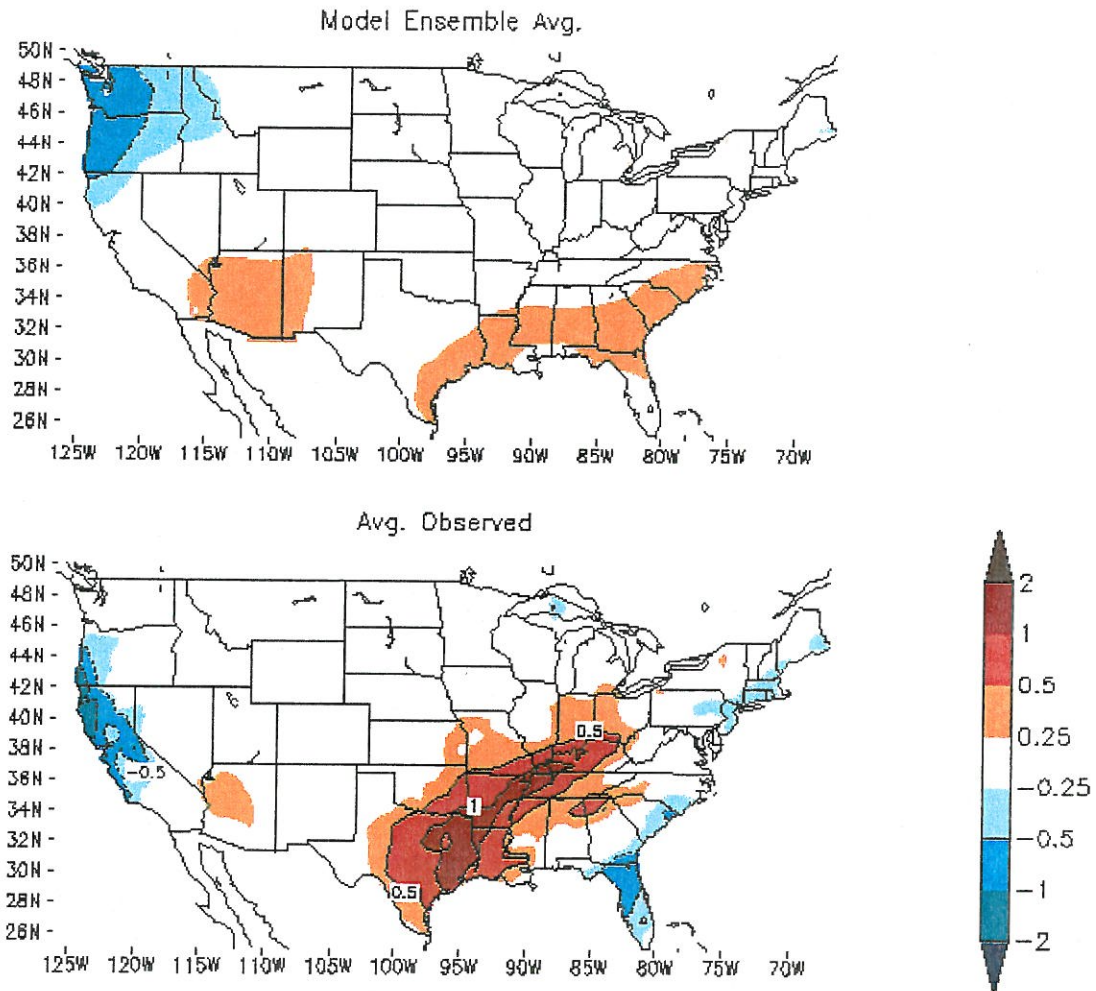
Figure 19. Average daily precipitation rate anomalies (mm/day) during AO positive events for model ensemble and observations. Positive regions are outlined with solid lines and negative regions outlined with dashed lines. The positive anomalies in eastern Texas and the Mississippi River valley and shifted in the model to the Deep South and into the Carolinas.
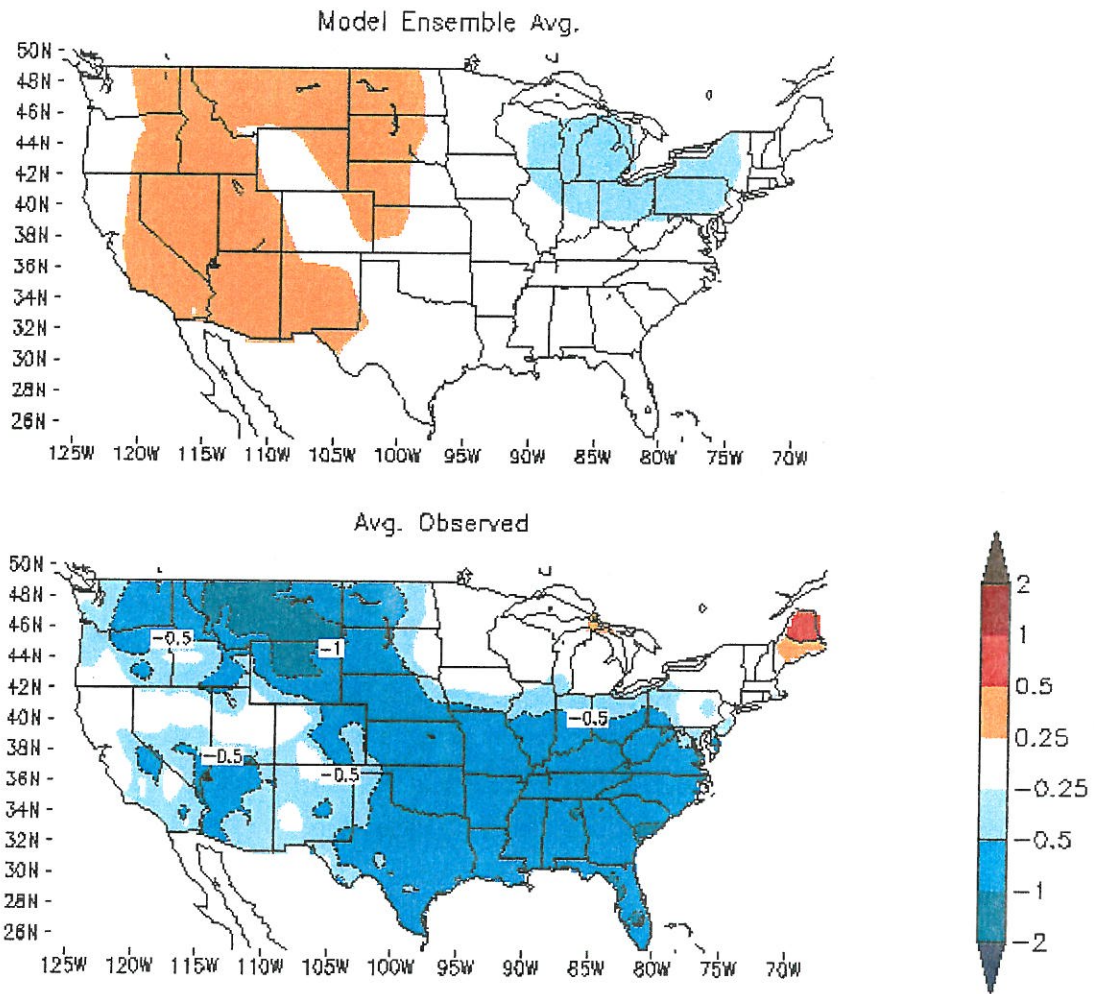
Figure 20. Average daily mean temperature anomalies (°C) during AO negative events for model ensemble and observations. Positive regions are outlined with solid lines and negative regions outlined with dashed lines. The model fails in producing the negative anomalies present over most of the country.
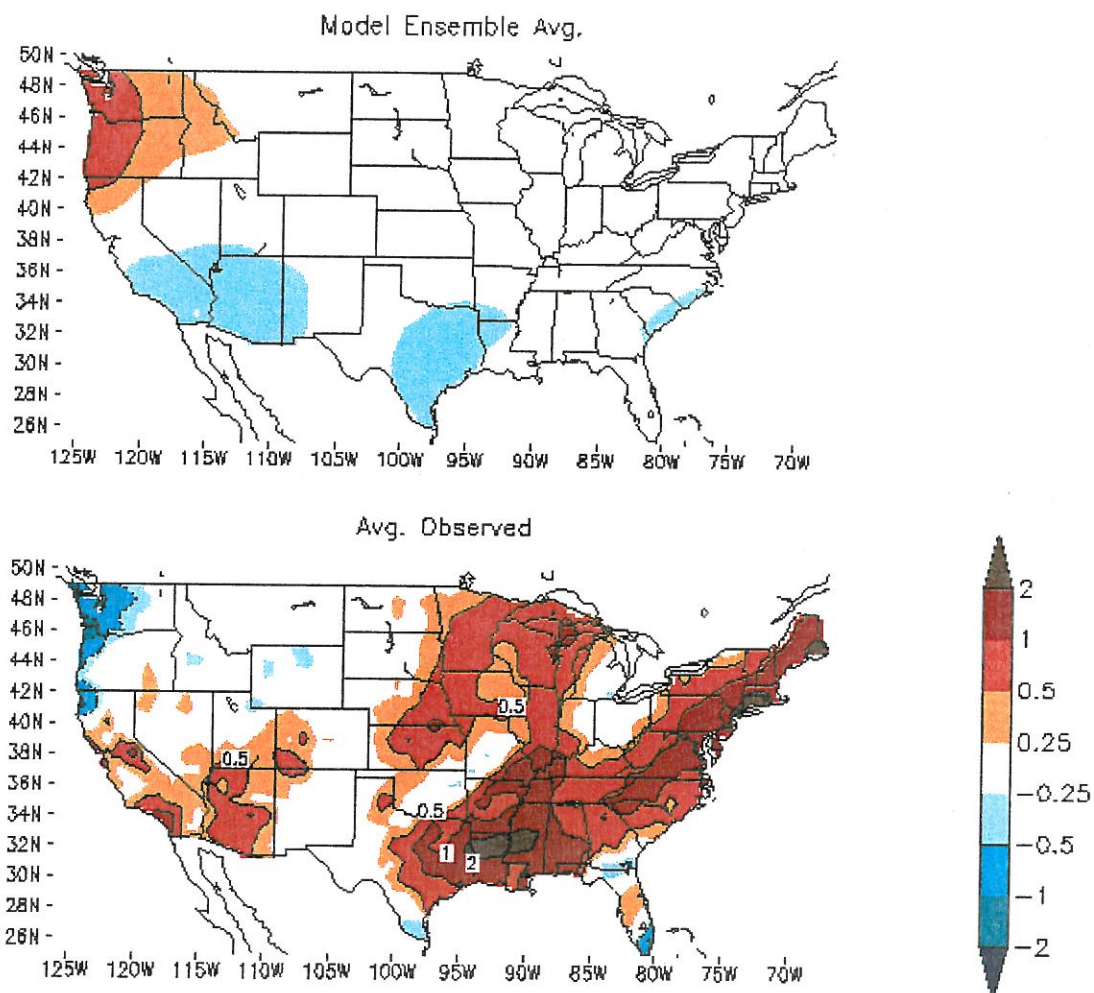
Figure 21. Average daily precipitation rate anomalies (mm/day) during AO negative events for model ensemble and observations. Positive regions are outlined with solid lines and negative regions outlined with dashed lines. The model fails to produce the positive anomalies present in the eastern half of the U.S.
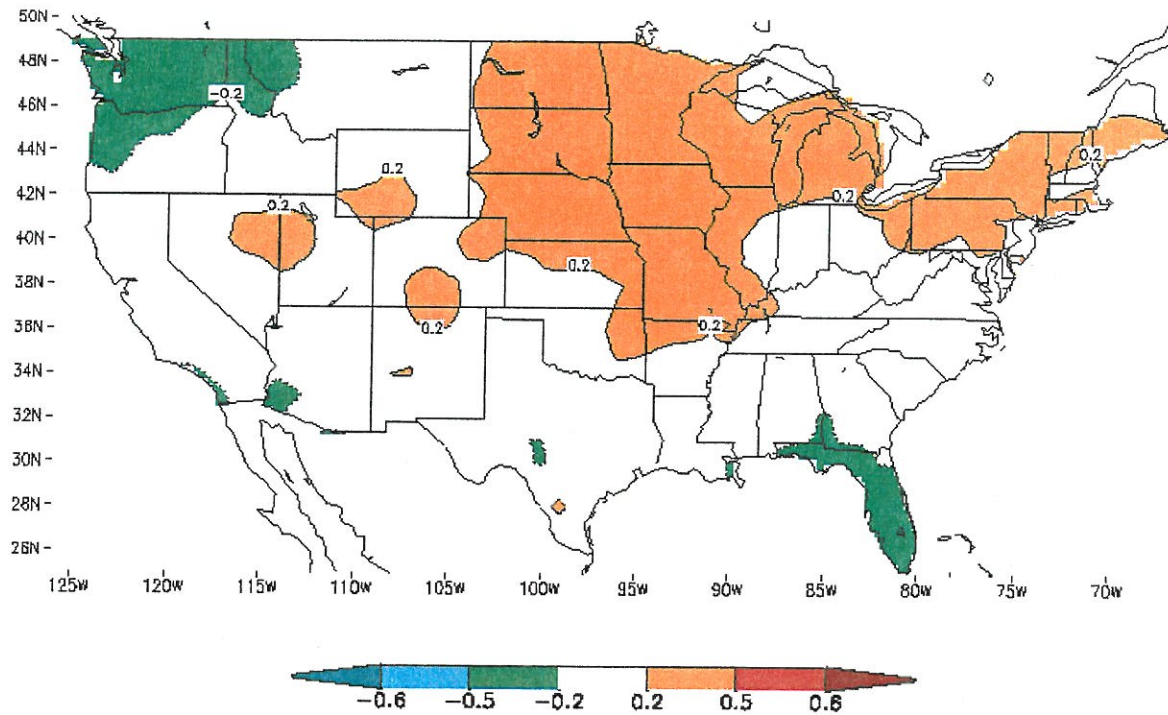
Figure 22. Distribution of temporal anomaly correlations of JFM seasonal mean temperature from 1979-1999. Regions of correlations of 0.5 or higher are areas in which the model demonstrates skill in predicting anomalies. Correlations of 1.0 represent perfect forecasts. Positive regions are outlined with solid lines and negative regions outlined with dashed lines. Positive anomaly correlations are located in the northern Great Plains and the Northeast, but all values are less than 0.5.
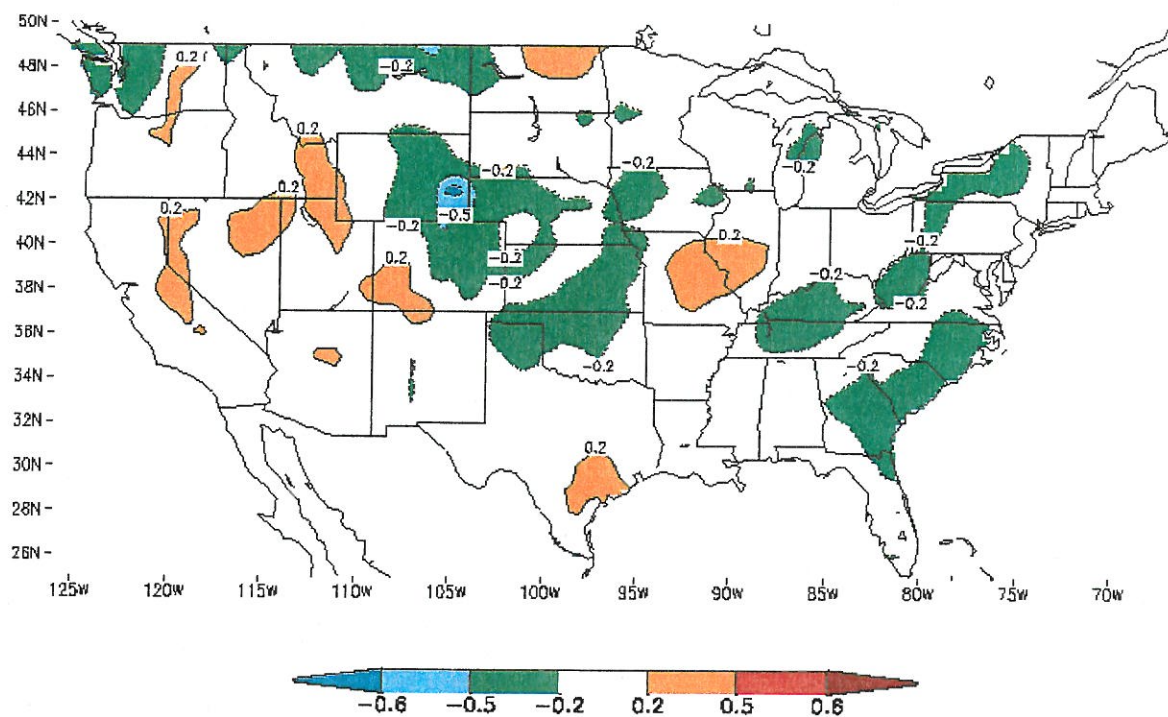
Figure 23. Distribution of temporal anomaly correlations of JFM seasonal precipitation rate from 1979-1999. Regions of correlations of 0.5 or higher are areas in which the model demonstrates skill in predicting anomalies. Correlations of 1.0 represent perfect forecasts. Positive regions are outlined with solid lines and negative regions outlined with dashed lines. There are no large regions of positive correlations, and no values greater than 0.5 are present.
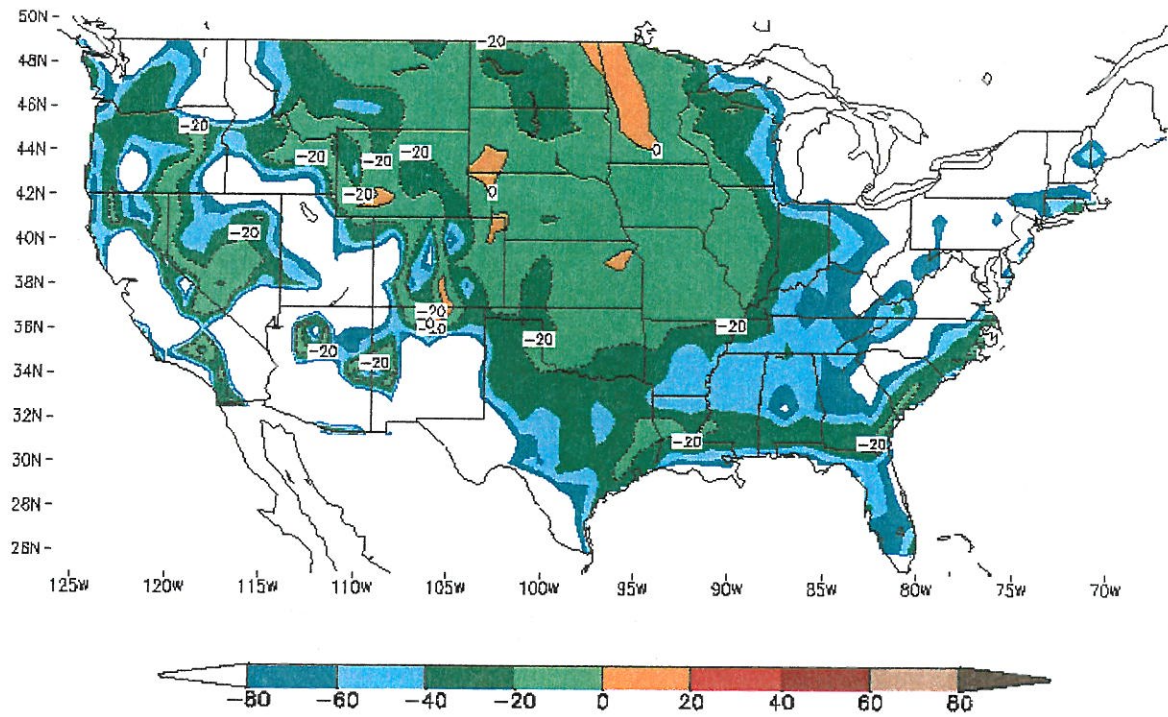
Figure 24. Skill score $(100 \cdot (1 - (\text{RMSE}_{\text{forecast}} / \text{RMSE}_{\text{clim}})))$ for seasonal mean temperature versus climatology. Values greater than zero are regions in which the model forecast is an improvement over climatology. Values are a percent improvement of the model over climatology. There are no large regions of values greater than zero.
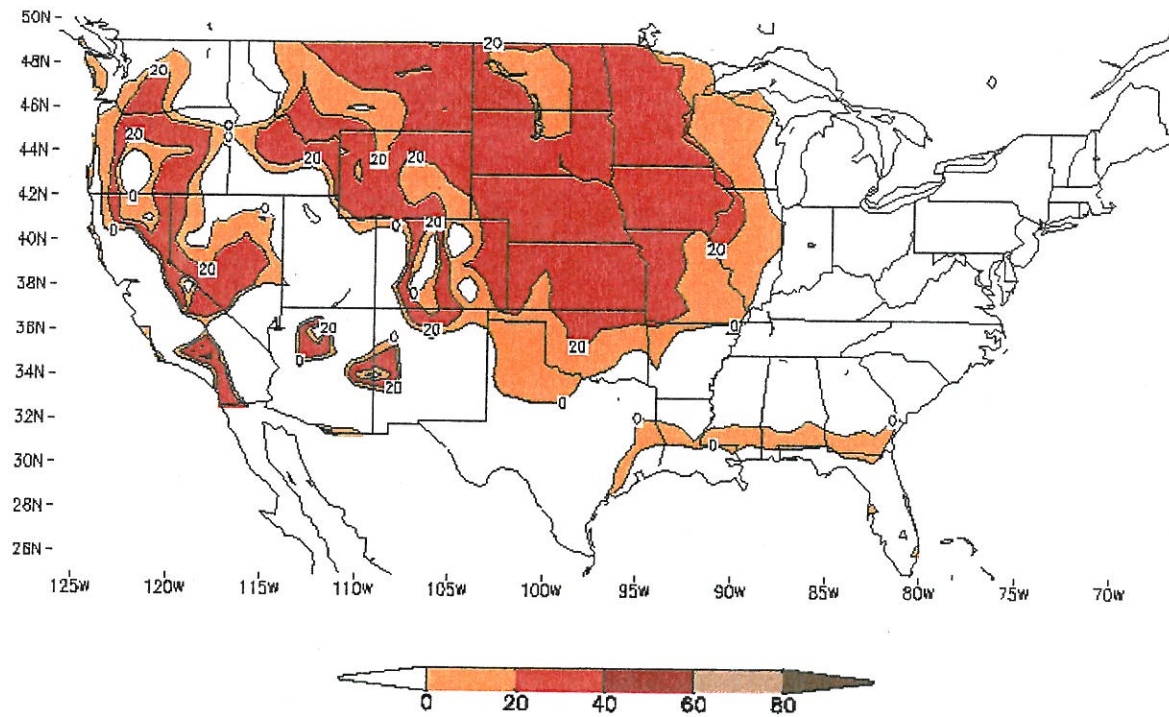
Figure 25. Skill score ($100 \cdot (1 - (RMSE_{forecast} / RMSE_{persistance}))$) for seasonal mean temperature versus persistence. Values greater than zero are regions in which the model forecast is an improvement over persistence. Values are a percent improvement of the model over persistence. Positive skill scores are located in the Central Plains and the Pacific Northwest.
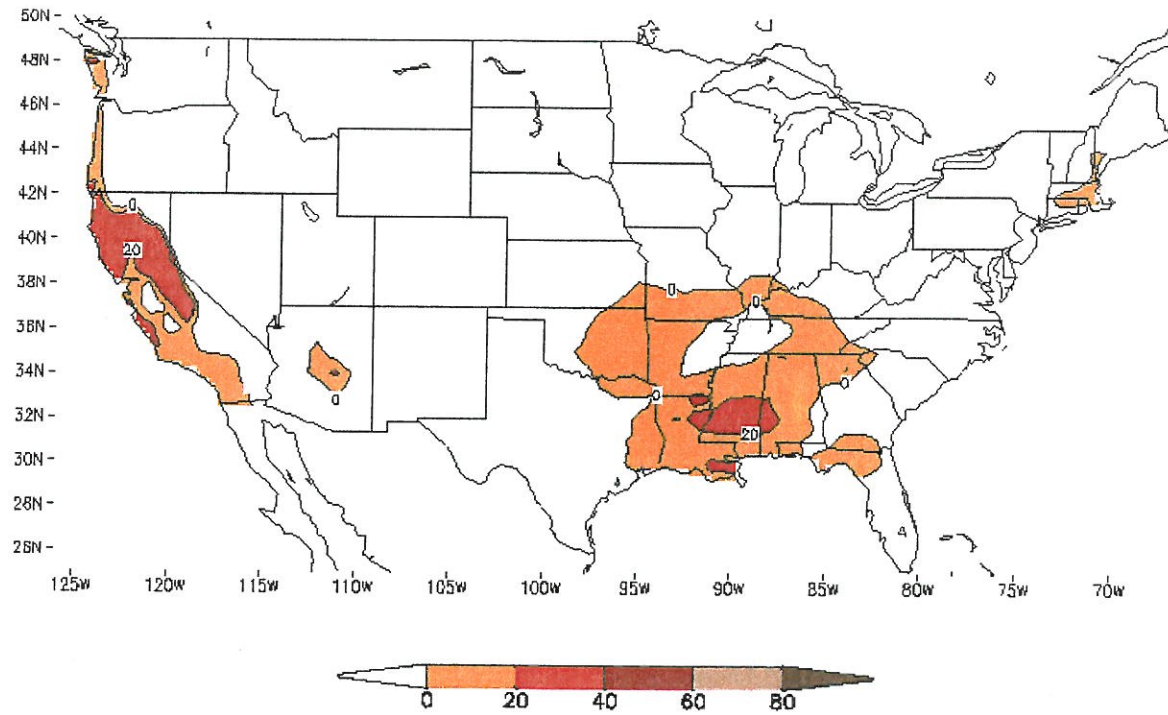
Figure 26. Skill score ($100 \cdot (1 - (RMSE_{forecast} / RMSE_{persistance}))$) for seasonal precipitation rate versus persistence. Values greater than zero are regions in which the model forecast is an improvement over persistence. Values are a percent improvement of the model over persistence. Positive regions are located along the northern Gulf Coast and California.

41

5. CONCLUSIONS AND DISCUSSION

The ability of a version of the NCEP operational climate prediction GCM to predict NH winter seasonal temperature and precipitation patterns over the U.S. was examined and assessed. The examination was based on the model's ability to produce, on average, the mean seasonal temperature and precipitation, as well as those associated with each phase of ENSO and the AO.

For mean temperature, the biases in the seasonal average are consistent with regions of highest RMSE indicating that the biases are fairly persistent, and therefore forecasts can be adjusted to include these biases. The model's ability to produce extreme events was poor. This fact is expected because the model has a low resolution and climate models are known to have less variance in their spread. The anomalies for temperature were negative at the warm extreme events and positive at the cold extreme events. Analysis of the extreme events and RMSE indicate that the biases are persistent throughout the spread. For precipitation, the model produced a positive bias everywhere except along the Pacific coast and along the northern Gulf states, where no anomalies were present. But these two regions had large RMSE and a lack of extreme events in the model indicating that the lack of extreme events may be responsible for the small biases in the mean.

42

Clearly, the most problematic result of this study is the model's very poor skill in predicting the effects of major climate events, namely ENSO and AO. Because ENSO and AO have their greatest influence on the U.S. during the winter season, the model's poor forecast ability is more troublesome.

On average, skill in predicting surface climate associated with ENSO events is limited. For individual events, the model was able to forecast one variable well, but the other variable for the same ENSO event was forecasted poorly. Model sensitivity to the SST boundary forcing may be responsible for the errors.

The inability to forecast patterns associated with AO shows that the model is unable to predict or maintain low frequency modes in the atmosphere. Large systematic errors, which distort the low frequency part of atmospheric variability, may be the reason for the lack of impact from atmospheric initial conditions. Errors in height anomalies and/or pressure fields poleward of 20° N, especially in the North Atlantic, may be responsible for the poor results.

Seasonal anomaly correlations were poor for both variables. In fact, no region shows a value greater than 0.5, which is the significance level for stating skill in the forecast. RMS skill scores calculated against climatology and persistence underscore the model's difficulties. Climatology is a better predictor than the model almost everywhere for mean temperature and everywhere for precipitation. The model does perform better than persistence over certain regions for both parameters. But, it is not as large or widespread of an improvement, as we would have hoped for in an operational model.

APPENDIX

Model Description

The GCM used in this study is the new version of the NCEP seasonal forecast model. The new dynamical prediction system was introduced in April 2000. A second generation of the model was made to further improve the coupled system to refine seasonal prediction.

The dynamical framework is based on the spectral AGCM described in Kanamitsu (1989). The reduced grid of Williamson and Rosinski (2000) was recently incorporated saving computer resources by about 30% at T62. The resolution is T62L28 meaning about 200 km horizontal resolution and 28 vertical layers.

The land model in the new system is based on the Oregon State University land model (Pan and Marht, 1987). Two soil layers are present and both soil temperature and water content are predicted. Canopy water content is predicted, and simple snow physics is also included.

The ocean model is a Pacific Ocean basin GCM covering the domain 45° S-55° N and 120° E-70° W. The horizontal resolution is 1.5° in the zonal direction, while in the meridional direction the resolution is 1/3° between 10° S-10° N and increases linearly to 1° between 10° and 20° N and S then 1° poleward of 20° N and S. The ocean model is coupled to a T42 (about 300 km) atmospheric model. In the coupling, the total SST from

the ocean is given to the atmosphere, and the momentum, heat, and fresh water fluxes from the atmosphere force the ocean model.

For atmospheric initial conditions, the model uses real-time T62L28 atmospheric analysis from the operational data assimilation (Kanamitsu, 1989). Both high and low frequency components of atmospheric initial conditions are incorporated. Some low frequency modes are incorporated. For land surface initial conditions, climatological soil wetness based on the NCEP/DOE Reanalysis-2 (Kanamitsu, et al., 2002, in press) is used.

The only boundary forcing in the hindcast runs analyzed in this study is from the observed SSTs. Therefore, the only difference in initial or boundary conditions between the ensemble members is in the atmospheric initial conditions.

For more information regarding the model and model processes please refer to Kanamitsu et al. (in press).

ACKNOWLEDGEMENTS

REFERENCES

Higgins, R. W., A. Leetmaa, Y. Xue, and A. Barnston, 2000. Dominant factors influencing the seasonal predictability of U.S. precipitation and surface air temperature. *Journal of Climate*, **13**, 3994-4017.

Kanamitsu M., 1989. Description of the NMC global data assimilation and forecast system. *Weather Forecasting*, **4**, 335-342.

Kanamitsu M., A. Kumar, J. Schemm, H. Juang, W. Wang, S. Hong, P. Peng, W. Chen, and M. Ji, (in publication). NCEP dynamical seasonal forecast system 2000. *Bulletin of the American Meteorology Society*.

Kanamitsu M., W. Ebisuzaki, J. Woolen, S. Yang, J. Hnilo, M. Fiorino, and J. Potter, 2002 (in press). NCEP/DOE AMIP-II Reanalysis (R-2). *Bulletin of the American Meteorology Society*.

Kumar, A., and M. P. Hoerling, 1995. Prospects and limitations of seasonal atmospheric GCM predictions. *Bull. of the Amer. Met. Society*, **76**, 335-345.

Kumar, A., and M. P. Hoerling, 2000. Analysis of a conceptual model of seasonal climate variability and implications for seasonal prediction. *Bulletin of the Amer. Met. Society*, **81**, 255-264.

Kumar, A., M. P. Hoerling, M. Ji, A. Leetmaa, and P. Sardeshmukh, 1996. Assessing a GCM's suitability for making seasonal predictions. *Journal of Climate*, **9**, 115-129.

Meehl, G. A., and B. A. Albrecht, 1991. Response of a GCM with a hybrid convection convection scheme to a tropical Pacific sea surface temperature anomaly. *Journal of Climate*, **4**, 672-688.

Palmer, T. N., and D. A. Mansfield, 1986. A study of wintertime circulation anomalies during the past El Nino events using a high resolution general circulation model. Part I: Influence of model climatology. *Quart. J. Roy. Meteor. Soc.*, **112**, 613-638.

Pan, H. -L. and L. Mahrt, 1987. Interaction between soil hydrology and boundary layer developments. *Boundary Layer Meteorology*, **38**, 185-202.

Rasmusson, E. M., and T. H. Carpenter, 1983. The relationship between eastern equatorial Pacific sea surface Temperatures and Rainfall over India and Sri Lanka *Monthly Weather Review*, **111**, 517-528.

Ropelewski, C. F., and M. S. Halpert, 1987. Global and regional scale precipitation patterns associated with the El Niño/Southern Oscillation. *Monthly Weather Review*, **115**, 1606–1626.

Ropelewski, C. F., and M. S. Halpert, 1989. Precipitation patterns associated with the high index phase of the Southern Oscillation. *Journal of Climate*, **2**, 268–284.

Thompson, D. W. J., and J. M. Wallace, 1998. The Arctic Oscillation signature in the wintertime geopotential height and temperature fields. *Geophysical Research Letters*, **25**, 1297-1300.

Thompson, D. W. J., and J. M. Wallace, 2000. Annular modes in the extratropical circulation. Part I: month-to-month variability, *Journal of Climate*, **13**, 1000-1016.

Wilks, D. S. 1995. Statistical Methods in the Atmospheric Sciences. Academic Press, San Diego, CA. 233-281.

Williamson, D. and J. Rosinski, 2000. Accuracy of reduced-grid calculations. *Quart. J. R. Met. Soc.*, **126**, 1619-1640.